Chemotaxis

Arwid Kuks

2021

Contents

Statement of Originality

This dissertation was written by me, in my own words, except for quotations from published and unpublished sources which are clearly indicated and acknowledged as such. I am conscious that the incorporation of material from other works or a paraphrase of such material without acknowledgement will be treated as plagiarism, according to the University Academic Integrity Policy. The source of any picture, map or other illustration is also indicated, as is the source, published or unpublished, of any material not resulting from my own research.

Summary

This dissertation was focused on building upon the pattern formation analysis performed and demonstrated for reaction-diffusion systems, applying methods used for these systems onto systems displaying chemotaxis, with a particular focus on variants of the Keller- Segel model as described in [12] for a certain set of parameters; as well as building upon the numerical methods used for modelling such systems and the procedures done to ensure the stability and accuracy of a given numerical method applied. In the course of this discertation, conditions for Turing pattern formation were obtained for three states of the Keller-Segel model, including one exhibiting non-constant chemotaxis. In addition, the isues surrounding two of these models were discussed, and were remedied.

In the following section, the numerical methods applied to model these systems were stated and derrived, with conditions for their stability being defined by use of appropriate stability analysis methods. Considered too was the accuracy of finite difference methods, especially for modelling advection, which led to the utilisation of a staggered grid finite volume scheme for the non-constant chemotaxis model, more specifically the two-step Lax Friedrichs method.

1 Introduction

1.1 Pattern formation

The modelling of pattern formation, biological or otherwise, is a problem that is of great interest in the literature, especially concerning biological processes such as the development of the embryo[20]. One may notice patterns everywhere in nature, such as in the development of sand dunes or basalt columns to name some non-biological cases, as well as biological cases such as the aforementioned embryo and tiger stripes; but if one considers the processes required for them to come about, they may seem unintuitive. The field of developmental biology is especially concerned with these processes for biological and chemical systems.

In this paper we are going to be looking at biological processes evolving over time and space, namely ones involving chemotaxis, and pattern formation which may arise from them. As such, it may be useful to summarise past work done in the preliminary discretisation [13], considering that some of the methods adopted for analysis and numerics of systems exhibiting Turing instability with simple diffusion will be applicable to systems exhibiting chemotaxis.

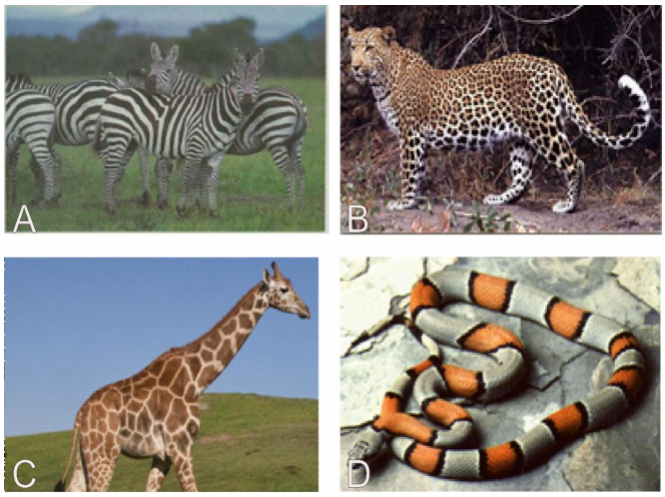

Figure 1: Examples of Turing pattern formation exhibited in animals, in alphabetical order: stripe pattern formation in zebra, spot patterns on a leopard, patch pattern formation on a giraffe and ring patterns formed on a coral snake [18] .

The previous discretisation [13] had focused on Turing instability, which is a process used to model biologically occurring pattern formation (for example on zebras on in embryos) .It was introduced with a summary of Turing's original paper [20]: where a descriptive model was created for describing how something like an embryo could develop into a more complicated creature, more specifically how could stable bands or points of chemical concentrations arise from what was initially considered a well mixed substance. Turing approached this by assuming the part evolving through time were based primarily on chemical processes, and adding a diffusion component on top of that. In addition to this, Turing had simplified the chemical interactions in the system, as the system in question would be affected by a great deal of hormones and genes, even if they themselves are less acted upon and assumed to be fully catalytic. Instead, they would be later accounted for in the system's kinematics. Therefore, for a 2 chemical system, the equations would take the following form:

$$A_t = F(A, B) + D_A \Delta A, \tag{1}$$
$$B_t = G(A, B) + D_B \Delta B. \tag{2}$$

In this context, the equations $F(A, B)$ and $G(A, B)$ represent the reaction part of the equation, and are called the kinetic terms of the equation, as they evolve over time rather than space. They may be thought of as driving the chemical interactions occurring within the system, hence the name. The terms inside the equations, A and B represent the chemical concentrations of the "morphogens", or the chemicals which are directly involved in pattern generation. Finally, D_A, D_B represent the diffusion coefficients for the diffusion terms to which they are attached. The diffusion component represents the natural dispersion of the chemical through the membrane on which it acts. Typically, D_A is taken to be 1, and D_B called d in the context of the previous dissertation. It should also be noted that in actuality, there are lots of catalysts, one sided reactions and side products often occurring at the same time as the primary reactions modelled, which should be taken note of when prescribing constants in the kinematics, even if the model doesn't address them explicitly. In addition, as our system is a system of PDEs, it is necessary to form boundary conditions which act upon our model. The model is taken with zero-flux boundary conditions, acting on the length of the membrane, L and at 0.

Turing also went on to state that the initial assumption should be made that the system is "well-mixed", or homogenous, that is to say that ΔA and ΔB should be assumed to be zero, and that the system should be stable for

those conditions. He also went on to say that this assumption would break down, and that another analysis should be performed, this time with diffusion and with instability occurring at some point. This analysis formed the backbone on the previous dissertation. Briefly covered too was the process of non-dimensionalisation, which made analysing systems easier. Finally, a numerical model was formed to describe the evolution of this system and to demonstrate the exhibition of Turing Instability patterns. As the system described before was non-dimensionalised, we should introduce also its non-dimensionalised general form, where u and v represent non-dimensionalised morphogen concentrations, $f(u,v), g(u,v)$ represent our kinetics and t is a non-dimensionalised variable representing our time component. In addition, as mentioned before, our D_A and D_B were set as 1 and d respectively. Also worthy of note is that in a "homogenous" state, the delta components would still be taken as zero.

$$u_t = f(u,v) + \Delta u,$$
$$v_t = g(u,v) + d\Delta v.$$

The analytics were began by considering a "well mixed" homogenous system. This part is relatively simple as we do not have to deal with the diffusion terms at all, and may treat this PDE system like an ODE to some extent for its stability analysis. Our first problem is finding the fixed points of the system, which we can do by setting its LHS to zero, and solving the resulting system of equations for viable u and v in terms of our parameters. For simplicity, we will call these fixed point values of u, v as u_0, v_0 respectively.

$$u_t = 0 = f(u_0, v_0),$$
$$v_t = 0 = g(u_0, v_0).$$

Having now obtained at least one fixed point about which we may continue our analysis, we linearise our system about the fixed point. If we consider only the kinetics of u_t, $f(x,t)$, their linearised form will take $f(u,v) \approx f(u_0,v_0) + uf_u(u_0,v_0) + vf_v(u_0,v_0)$. The $f(u_0,v_0)$ term is then eliminated, as by definition of the stable points for the homogenous state, the kinetics must be equal to zero. The same process is applied to $v_t = g(u,v)$, but will be skipped for brevity. We then derived our Jacobian (a matrix of derivatives of u and v for f and g), which left us with the following matrix, where our derivatives had the fixed points derived earlier substituted into them:

$$J = \begin{pmatrix} f_u & f_v \\ g_u & g_v \end{pmatrix}.$$

We may now find the stability of this system, which we do by introducing a stability parameter λ, and finding conditions when the following matrix equation has $\lambda < 0$, which corresponds to a stable system: $|J - \lambda I| = 0$. Having achieved this, we found that we would have two conditions for stability of the homogenous state, those being: $f_u + g_v < 0$, and $(f_u g_v - f_v g_u) > 0$. This part is essential in the analysis as it gives us conditions which must be held to during the analysis of the distributive system in order to prevent it from being completely unstable.

Having done this, we now consider the "distributive" system, that is the actual case where diffusion is assumed to have an impact. The assumptions made in order to arrive at the "homogenous" model can not be maintained for long as the system evolves in time and space. For instance, some small differences in concentrations over the medium exist. However, some of the results received from the "homogenous" analysis may be directly applicable to our distributive system, namely our derived conditions and our fixed point parameters.

As the system has spatial components affecting it now, it may not be purely analysed like an ODE system, and getting it to a state where it could be had been a relatively heavy component of the 552 dissertation. As such, it will be covered here in some more detail. First off, we need to linearise about our fixed point once more, this time admitting functions in both time and space. Let us call the linear functions substituted $\xi(t, x)$ and $\delta(t, x)$, such that our linearisation gives: $u = u_0 + \xi(t, x)$, $v = v_0 + \delta(t, x)$. Note that partial differentiation of these terms in order to substitute them into the equation system eliminates the constant term about which linearisation took place.

Having constructed our linearisation terms, we substituted them into our distributive equation system to arrive at a linearised system of partial differential equations, after also linearising f and g:

$$\begin{aligned}\xi_t =& \xi_{xx} + f_u\xi + f_v\delta,\\ \delta_t =& d\delta_{xx} + g_u\xi + g_v\delta.\end{aligned}$$

As is evident by looking at the linearised system derived here, one of our major problems is that it is still a partial differential system of equations. In order to solve this, we will enter a substitution for ξ and δ, where we separate them into an infinite series of multiples of two single-term equations. For brevity, only ξ will be demonstrated here, however the exact same principles

apply to δ:

$$\xi = \sum_{i=0}^{\infty} \xi_i^{(1)}(t)\xi_i^{(2)}(x).$$

By making this substitution, we can approximate $\xi_i^{(2)}(x)$ by the sum of the sine and cosine of $\frac{\pi i x}{L}$, where L is the length of our medium. As we apply zero-flux boundary conditions, we may eliminate the sine component, leaving us with $\xi_i^{(2)}(x) = cos\left(\frac{\pi i x}{L}\right)$, which simplified our linearised system of partial differential equations into an infinite number of ODE systems, for $i \in \mathbb{N}_0$. In real terms, this is directly proportional to our wave number, k, which we define as $k = \frac{i\pi}{L}$. In order to prepare the system for the next part of our analysis, it can be represented as a matrix equation:

$$\begin{pmatrix} \dot{\xi}_i \\ \dot{\delta}_i \end{pmatrix} = -k^2 \begin{pmatrix} 1 & 0 \\ 0 & d \end{pmatrix} \begin{pmatrix} \xi_i \\ \delta_i \end{pmatrix} + \begin{pmatrix} f_u & f_v \\ g_u & g_v \end{pmatrix} \begin{pmatrix} \xi_i \\ \delta_i \end{pmatrix}.$$

From this point on, we can take the Jacobian and solve it for a range of unstable cases for some k , while keeping to the conditions necessary for the homogenous state to be stable. These conditions were found to be the following in the course of the dissertation: $df_u + g_v > 0$ and $(f_u g_v - f_v g_u) < \frac{(df_u + g_v)^2}{4d}$. The dissertation also describes obtaining the wave number at which the system becomes unstable. Finally a simple PDE simulation was used, namely the Euler method, to demonstrate the results obtained.

In [13] two specific models were analysed with respect to pattern formation: the Schnakenberg model and the Meinhardt model. Not covered however were their biological applications, nor what their terms sought out to model and describe. It may therefore be valuable to cover this here.

The Schnakenberg model is a reaction-diffusion model designed to involve as minimal a number of reactants and reactions as feasible, while being able to exhibit limit cycle behaviour and be applicable to chemical problems [2]. To this end, Schnakenberg found that at least 3 reactions would need to be taking place for his model to work as intended, with one being "autocatalytic", that is for two chemicals A and B, the reaction taking place between A and B would result in only B being produced [2]. The terms of the equation therefore correspond to the relative concentrations of chemicals as they are produced and recycled. For the model considered by [13], only the concentrations of two chemicals were considered.

The Meinhardt model, or Geirer-Meinhardt model is an activator-inhibitor

model, that is to say a model where the two chemicals involved work in opposition to another. These models are a subset of reaction-diffusion models, discovered by the same [9]. Activator-inhibitor models, and specifically the Meinhardt model, are used to describe the formation of chemical and biological patterns, including those of animals such as stripes and spots [10].

1.2 Chemotaxis

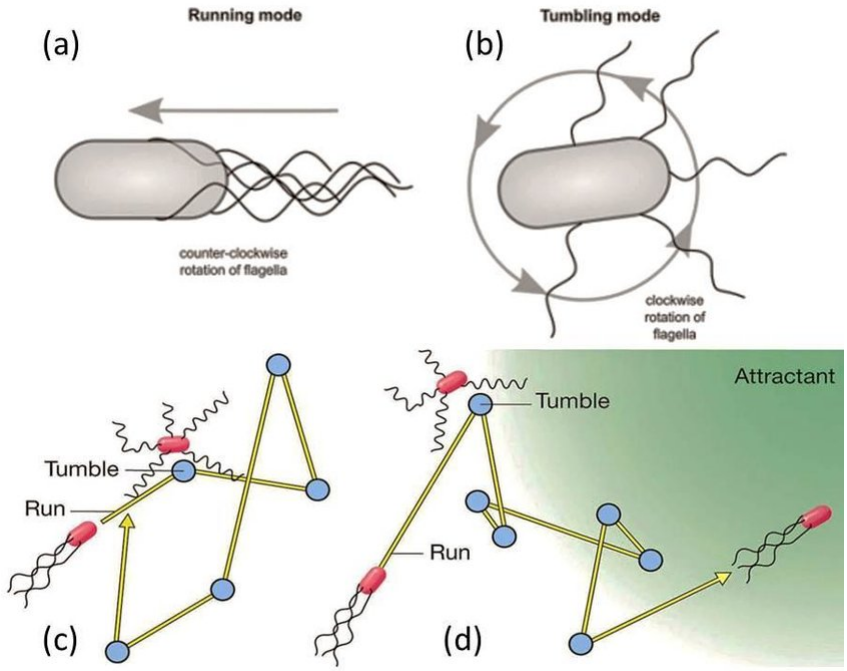

Figure 2: An illustration of an E. coli bacterium and the mechanism by which it is able to move. In alphabetical order: counter-clockwise flagellum spin (forward movement), clockwise flagellum spin(tumbling mode), random movement of an E.coli bacterium without chemical stimulus, movement of an E.coli bacterium with a positive chemical stimulus [6].

The process that we will follow for the analysis of our system describing chemotaxis is relatively similar to that which was followed for the analysis of Turing instability formation in [13], although more on the different challenges inherent in these systems will be described in greater detail later on. A brief summary of the methods involved has been provided in the previous section as well.

Chemotaxis is a behaviour exhibited by certain cells and single-celled organisms where they respond to a chemical stimulus such as a pheromone or a poison. Consider a bacterium of a certain species. That bacterium will require some food to survive or perhaps also be able to avoid threats, and in order to do that, it will need a mechanism by which it can detect higher concentrations of the food and move towards it, or be able to detect threats from afar and avoid them. These processes are examples of chemotaxis, be that to positive stimuli such as the food, or to a negative stimuli such as a poison. Although the exact processes of chemotaxis vary by what kind of organism is undertaking it (eukaryotic vs prokaryotic), the constant remains that the process is based upon proximity to the chemical stimulus, more specifically, the chemical gradient.

Sticking with bacteria for now, we may consider a real world example of an E. Coli bacterium. The E. Coli bacterium has little "tails" to aid its movement, called flagella. These flagella can move in two directions: clockwise or anti-clockwise, from the perspective of someone looking down the flagella towards the bacterium. If they move anti-clockwise, the flagella will align relatively straight, and the bacterium will move forward. If the flagella move clockwise however, they will bundle apart, and the bacterium will move relatively little, instead rotating or "tumbling" [21]. The bacterium will switch between the two states when no chemotaxis is taking place at a steady rate, thus allowing the bacterium to wander aimlessly if no stimulus is to be found [3]. However, if a stimulus is found, the bacterium will change the rate at which it switches, depending on whether it's going towards or away from the stimulus, and whether the stimulus is positive or negative, enabling the bacterium to move to more favourable locations [4]. This behaviour is illustrated in 2.

As mentioned before, chemotaxis is also exhibited in eukaryotic cells, which are ones with a defined nucleus (such as those found in the animal kingdom), albeit it is exhibited in oftentimes more complex ways, owing to the different circumstance that these cells find themselves in, such as greater size, multi-cellular structures and so on. A perhaps apt example (given the focus of Turing's paper on embryonic growth) of this may be the utilisation of chemotaxis by sperm cells to reach the egg, although as with morphogenesis and Turing patters, other important examples arise as well. For instance, in the medical field chemotaxis plays a role in the modelling of many diseases and ailments, even putting aside bacterial chemotaxis, improper chemotaxis of certain cells like leukocytes and lymphocytes plays a role in inflammatory diseases like asthma and arthritis [8] [17]. In addition to this, the natural

process of chemotaxis in a body may become subverted during cancer metastasis [19]. Because of the role that chemotaxis plays in all this, its study and modelling is important for mathematical biology.

Eukaryotic cells are often times quite a lot larger larger than prokaryotic cells. Because of this, they can benefit from being able to sense differences in concentrations between two separate points [11]. This removes the need to "run and tumble" as the E. coli has to make do with, however it does create the need for a "dynamic and polarised distribution of receptors" [11]. Triggering these receptors with a chemical gradient will result in movement towards or away from the chemical, depending on whether it is a positive stimulant or negative. As stated in the last paragraph, the role which chemotaxis plays is key in biology, with deployment of mathematical models and techniques to describe it ever increasing. For instance, chemotaxis is being used in describing the development of an embryo.

Relating this all back to our Turing system however, the key difference between the two classes of system when it comes to the mathematics is that Turing reaction-diffusion systems only have one spatial component per equation: the diffusion component which is always the ∇^2 of the concentration which the LHS represents the first time differential of, multiplied by some constant.

However, for chemotaxis, there is no such limitation. The spatial component may include a ∇^2 of another concentration, it may also be a ∇ of this concentration and the ∇ of another concentration, for example. As such, not much changes in the homogenous portion of our analysis, except for different models having different kinematics, but for our distributive system the matter of finding appropriate linearisations may prove more tricky. In addition to this, some combinations of ∇ are difficult to model numerically, which is why alternative schemes are covered further on for modelling such systems numerically.

More specifically, the chemotactic system that this dissertation is concerned with is the Keller-Segel model, introduced by Keller and Segel in the 1970's [12]. Though a more general form of this system will be described in detail further on, a simplified example shall first be presented for digestibility purposes. By taking the Keller-Segel system from [12] and having $\Psi(u, v) \equiv 1, \Phi(u, v) \equiv \alpha$ for all admissible values of u and v, we are left with the

following system:

$$u_t = d_u \nabla^2 u - \alpha \nabla^2 v + k_3(u, v), \tag{3}$$
$$v_t = \nabla^2 v + k_4(u, v)u - k_5(u, v)v, \tag{4}$$

where d_u is a constant of diffusion, α a constant of chemotaxis and k_3, k_4, k_5 are the kinetics of the system.
The general version of this system is the following:

$$u_t = \nabla \cdot (d_u \Psi(u, v) \nabla u - \Phi(u, v) \nabla v) + k_3(u, v), \tag{5}$$
$$v_t = \nabla^2 v + k_4(u, v)u - k_5(u, v)v, \tag{6}$$

where u and v denote cell population density and the concentration of a positive chemical stimulant. Additionally, $\Phi(u, v)$ represents the cell's chemotactic sensitivity, $\Psi(u, v)$ represents the diffusivity of the cells, $k_3(u, v)$ denotes the death and growth of the cells, $k_4(u, v)$ denotes the production of the chemical stimulant while $k_5(u, v)$ denotes its degradation. Finally, d_u represents the diffusion coefficient of the cell [1]. For the purposes of our further analysis, we will introduce the following constants $k_4(u, v) = \beta$ and $k_5(u, v) = \gamma$.

Additionally, depending on whether the system exhibits logistic growth or not, $k_3(u, v)$ will either be equal to $\rho u(\delta - u)$ or zero respectively. Finally, for systems with constant chemotaxis, $\Psi(u, v)$ and $\Phi(u, v)$ will equal 1 and α respectively, otherwise $\Phi(u, v) = \alpha u$. α, ρ, δ are all constants.

2 Modelling pattern formation due to chemotaxis

2.1 Keller-Segel Model

The first model that we call consider is a simple case of the Keller-Segel model, with kinetic terms $k_3 = 0$, $k_4 = \beta$ and $k_5 = \gamma$, as well as with chemotactic sensitivity $\Phi(u, v) = \alpha$:

$$A_t = d_u \nabla^2 A - \alpha \nabla^2 B, \tag{7}$$
$$B_t = d_v \nabla^2 B + \beta A - \gamma B. \tag{8}$$

Such a model would have a cell population influenced only by chemotaxis, due to the kinetic for death and growth of the cells being always zero, as well as having constant chemotaxis, irrespective of cell population density. In this section, our first concern with this system will be to non-dimensionalise it, which will aid with analysis of the system later on. To do this, we introduce non-dimensionalisation constants and derive further substitutions from them:

$$u = AP, \tau = RtL^{-2}, \qquad u_\tau = \frac{L^2 P}{R} A_t, \qquad \nabla^2 A = \frac{1}{PL^2} \nabla^2 u, \tag{9}$$
$$v = BQ, \chi = xL^{-1}, \qquad v_\tau = \frac{L^2 Q}{R} B_t, \qquad \nabla^2 B = \frac{1}{QL^2} \nabla^2 v. \tag{10}$$

The constants introduced here are P, Q, R, L, for which we will find appropriate solutions such as to eliminate up to 4 constants from the original equation system, although this number will be found to be lower in practise. The non-dimensionalised variables introduced: u, v, τ, χ, represent the cell population density, concentration of positive chemical stimulant, time and space respectively. It should also be noted that ∇^2 with respect to u and v has also been non-dimensionalised by the above scheme. Having constructed our non-dimensional terms, we substitute them into our equation system to obtain the following:

$$u_\tau = \frac{d_u}{R} \nabla^2 u - \frac{\alpha P}{QR} \nabla^2 v, \tag{11}$$
$$v_\tau = \frac{d_v}{R} \nabla^2 B + \frac{\beta L^2 Q}{PR} u - \frac{\gamma L^2}{R} v. \tag{12}$$

Given this system, we are able to now pick our 4 non-dimensionalisation constants to simplify down the system. We may start by making the substitution $R = d_v$ and introducing a diffusion constant $D = \frac{d_u}{d_v}$, which will simplify our

diffusion as much as it can be simplified. We may then focus on the kinetics of the system, as make the substitution $L^2 = \frac{d_v}{\gamma}$, which will reduce the coefficient of the degradation of our chemical stimulant to 1. We will then be left with two non-dimensionalisation constants P and Q, however in both circumstances where they remain, one is divided by the other. In effect, this means that we are given only 1 degree of freedom to make substitutions for elimination. The substitution chosen is $\frac{P}{Q} = \frac{\beta}{\gamma}$, which reduces the coefficient of the production of our chemical stimulant to 1. Finally, we group the constant coefficients of the chemotaxis into one overall non-dimensional variable: $a = \frac{\alpha\beta}{d_v\gamma}$.

Having obtained a non-dimensional form of this model, shown below, we now move onto analysing it for pattern formation. For convenience, the non-dimensionalised parameters τ and χ have been replaced with t and x respectively.

$$u_t = D\nabla^2 u - a\nabla^2 v, \tag{13}$$

$$v_t = \nabla^2 v + u - v. \tag{14}$$

We now make the assumption that our system is homogenous. Materially speaking, this assumption posits that our system starts off well mixed, with negligible differences in concentration over the medium. In practise, this means that we may assume our chemotactic and diffusion parameters to be zero, leaving us with just the kinetics of the system:

$$u_t = 0, \tag{15}$$

$$v_t = u - v. \tag{16}$$

In order to find stable homogenous solutions for the system, we must first find the stable points of the system. This is done by finding the appropriate values of u and v when $u_t, v_t = 0$. As such, we set the left-hand side of 15 to zero as follows:

$$u_t = 0 = 0,$$
$$v_t = 0 = u_0 - v_0.$$

This system is very trivial to solve for an appropriate solution for our fixed point. Namely, the solution is a set of points where $v_0 = u_0$.
Having found the fixed points, we may now move onto solving for stability. To do this, we take the Jacobian matrix of 15 and subtract from it the eigenvalue identity matrix, where λ is the eigenvalue:

$$\begin{vmatrix} -\lambda & 0 \\ 1 & -1-\lambda \end{vmatrix} = 0.$$

We then solve this equation for λ, which returns us with two possible solutions: $\lambda = 0, -1$. In order for the homogenous system to be stable, $\lambda < 0$ therefore we are left only with $\lambda = -1$ as a possible solution. This solution is independent of any constants, therefore it is satisfied in all cases.

Having finished our homogenous analysis, we now move onto the distributed analysis part. We begin by making a linear substitution, introducing ξ and δ for u and v respectively (and although these were not present, eliminating all terms of second order or greater). This leaves us with the following system, given that the medium has only one spatial dimension:

$$\xi_t = D\xi_{xx} - \delta_{xx},$$
$$\delta_t = \delta_{xx} + \xi - \delta.$$

Next we make a substitution for ξ and δ of $\xi(x,t) = \sum_{i=1}^{\infty} \xi^{(t)}(t) cos(\frac{\pi i x}{L})$ and $\delta(x,t) = \sum_{i=1}^{\infty} \delta^{(t)}(t) cos(\frac{\pi i x}{L})$. In essence, we split up the terms into two: a time component and a spatial component. From here, it is evident that the spatial component will have a solution in terms of sines and cosines, and we can eliminate the sines by our zero flux boundary conditions. Having obtained this system, we cancel out the $cos(\frac{\pi i x}{L})$ turning our PDE system into infinitely many ODE systems, for $i \in \mathbb{N}^+$. We also simplify our notation of $\xi^t(t)$ and $\delta^{(t)}(t)$ to $\xi(t)$ and $\delta(t)$, as well as letting $k = \frac{i\pi}{L}$, where k is the wave number of our system:

$$\dot{\xi} = Dk^2\xi - k^2\delta, \tag{17}$$
$$\dot{\delta} = k^2\delta + \xi - \delta. \tag{18}$$

As we did for the homogenous system, we take the Jacobian of the above yielding us the following equation for λ:

$$\lambda = \frac{k^2(D+1)+1}{-2} \pm \frac{\sqrt{(Dk^2+k^2+1)^2 - 4h(k^2)}}{2}, \tag{19}$$
$$h(k^2) = (Dk^2)(k^2+1) - ak^2. \tag{20}$$

From the above equation, we want to obtain a result for λ which is positive for at least one of the roots. Inspecting the term outside of the square root, we note that by conditions derived for the homogenous system, the term will remain negative for all values of k^2. Therefore the square root term must be greater than the term outside the square root for some λ, and in order for that to be the case, $h(k^2) < 0$ is required, which gives us the following required condition:

$$D(k^2+1) < a. \tag{21}$$

If we consider our definition of k, namely $k = \frac{i\pi}{L}$ where L represents the length of the medium upon which our morphogens interact, we can further simplify this resulting condition. For situations where the length of the medium is large, that is $L \to \infty$, our value for k must subsequently approach zero for a given value of i. As a result, we are left with $D < a$ as a simplified approximate condition for cases where the medium of morphogen interactions is very large. In order to avoid this in simulations, a relatively small medium size of $L = 20$ was chosen.

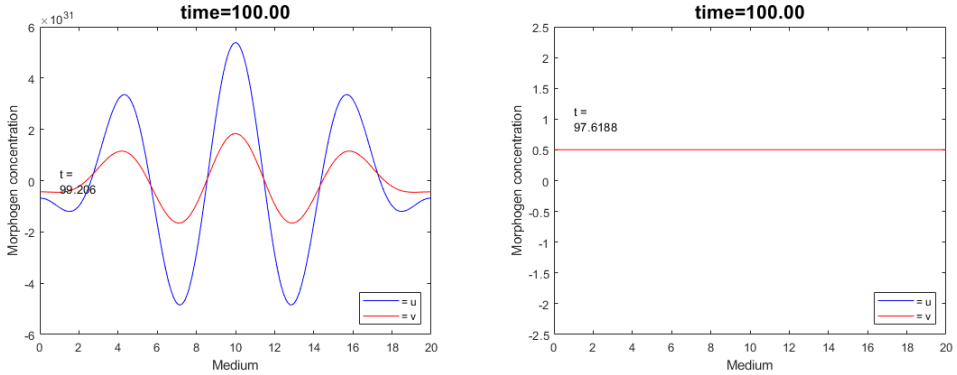

Figure 3: Two simulations of morphogen concentrations over time. For the first simulation, on the left, the conditions for Turing instability are met, therefore the system exhibits characteristic stripes. The peaks demonstrated here are increasingly tall, which would imply unchecked concentration growth. Further issues are exhibited in the fact that much of the concentrations are negative, which is inconsistent with observed reality. Parameters are $a = 5, D = 3$. For the second simulation, the conditions are not met and therefore no pattern development occurs. Parameters are $a = -2, d = 5$.

Observing the figure, it becomes apparent that as time progresses, morphogen concentration rises very quickly, overcoming our original disturbances by orders of magnitude. In addition, the concentrations are below zero for some parts of the graph, which is something that should be avoided as concentrations of morphogens can not be negative. These two occurrences are something which obviously does not occur naturally, and they are a consequence of a lack of kinetics in u_t, which leads to the growth of u_t being relatively unchecked, beyond chemotaxis and diffusion, both of which are inadequate to control its growth. As such, we should consider introducing a non-zero term for k_3 to make the growth and decay remain confined to a certain range. This is the role that the term serves in the model, representing the growth and decay of the cell population density. We will do this by introducing a lo-

gistic term in the next subsection, which should help keep the cell population density within a certain range.

2.2 Keller-Segel with logistic growth

In order to deal with the cell population problem, we will choose a different function for the k_3 term, representing the growth and death of the cells. The function chosen is a logistic function, introducing the dimensional parameters ρ and δ, in terms of the cell population density. The other terms were kept the same :

$$A_t = d_u \nabla^2 A - \alpha \nabla^2 B + \rho A(\delta - A), \tag{22}$$

$$B_t = \nabla^2 B + \beta A - \gamma B. \tag{23}$$

As done in the previous example, we first will non-dimensionalise the system before proceeding onto analysing it for pattern formation. We will introduce the non-dimensionalisation constants in the same way as before, along with their derivations:

$$u = AP, \tau = RtL^{-2}, \qquad u_\tau = \frac{L^2 P}{R} A_t, \qquad \nabla^2 A = \frac{1}{PL^2} \nabla^2 u, \tag{24}$$

$$v = BQ, \chi = xL^{-1}, \qquad v_\tau = \frac{L^2 Q}{R} B_t, \qquad \nabla^2 B = \frac{1}{QL^2} \nabla^2 v. \tag{25}$$

The non-dimensionalisation constants here are P, Q, R, L which will enable us to eliminate up to 4 constants from 22. u and v correspond to A and B respectively (with their respective ∇ also being non-dimensionalised), as do τ and χ to t and x respectively. We may now substitute them into 22, having found our non-dimensionalisation constants, to give us the following:

$$u_\tau = \frac{d_u}{R} \nabla^2 u - \frac{\alpha P}{QR} \nabla^2 v + \frac{L^2 \rho}{PR} (\delta P - u) u, \tag{26}$$

$$v_\tau = \frac{d_v}{R} \nabla^2 v + \frac{\beta L^2 Q}{PR} u - \frac{\gamma L^2}{R} v. \tag{27}$$

We can now begin to choose dimensionally appropriate substitutions for our non-dimensionalisation constants. Let us first focus on the logistic term. We can easily eliminate δ by choosing $P = \delta^{-1}$, as δ only appears once in the entire system. Focusing now on the diffusion terms of the system of equations, we can only eliminate one of d_u and d_v by choosing an appropriate R. As such, we decide to eliminate d_v by choosing $R = d_v$, and introducing the non-dimensional diffusion ratio $D = \frac{d_u}{d_v}$.

The next 2 selections focus primarily on the v_τ kinetics. By making having the $L^2 = \frac{d_v}{\gamma}$ we can eliminate the coefficients of v. We are then left with only one non-dimensionalisation parameter, Q, for which we make the following substitution: $Q = \frac{\gamma}{\beta\delta}$.

We are now left with no more non-dimensionalisation constants to assign values to, however we can group up the constants which we have left, simplifying our system with no loss of generality. These constants are the non-dimensional chemotactic parameter, $a = \frac{\alpha\beta}{d_v\gamma}$ and the non-dimensional logistic growth and decay strength parameter $b = \frac{\rho\delta}{\gamma}$. We will now also drop the τ and χ in favour of t and x.

$$u_t = D\nabla^2 u - a\nabla^2 v + bu(1-u), \tag{28}$$
$$v_t = \nabla^2 v + u - v. \tag{29}$$

Having obtained a non-dimensional system of equations, we now proceed with pattern formation analysis. First we will make the homogeneity assumption and presume that our chemotactic and diffusive terms have negligible impact:

$$u_t = bu(1-u), \tag{30}$$
$$v_t = u - v. \tag{31}$$

For the homogeneity part of this analysis we must find the conditions required to ensure the system is stable. However, we must first find the fixed points to analyse the stability of. This is relatively simple, as we can find them by requiring $u_t, v_t = 0$:

$$u_t = 0 = bu_0(1-u_0),$$
$$v_t = 0 = u_0 - v_0.$$

This gives us two point-solutions for the fixed points, namely $u_0 = 1, 0$, $v_0 = 1, 0$.
Having found fixed points to perform stability analysis on, we now take the Jacobian of the homogenous system, namely:

$$\begin{vmatrix} b - 2ub - \lambda & 0 \\ 1 & -1 - \lambda \end{vmatrix} = 0,$$

and arrive at the following conditions for λ:

$$\lambda = \frac{b - 2u_0 b - 1}{2} \pm \frac{\sqrt{(b - 2u_0 b - 1)^2 + 4b(1 - 2u_0)}}{2}. \tag{32}$$

From the above system, we substitute our fixed point values to analyse them for stability. The requirement for stability is that both λ solutions must be less than zero.

$$
\begin{aligned}
&u_0 = 0 : \\
&\qquad \lambda = \frac{b-1}{2} \pm \frac{\sqrt{(b-1)^2 + 4b}}{2}; \\
&u_0 = 1 : \\
&\qquad \lambda = \frac{-b-1}{2} \pm \frac{\sqrt{(b+1)^2 - 4b}}{2}.
\end{aligned}
$$

By inspection we notice that in order to have $\lambda < 0$, the square root term has to be less than the term outside, therefore the second term in the square root must be negative, which is impossible if $u_0 = 0$. Therefore we reject the stable point at $(u, v) = (0, 0)$ from our analysis, and from now on use the substitution $u_0 = 1$ exclusively . For this fixed point stability is assured so long as $b > 0$, which is already an assumption being made.

Having concluded out homogenous analysis of the system, we now move onto the distributed analysis part. The reason is that our homogeneity assumption does not hold, requiring us to consider the dimensional terms, namely the chemotactic and diffusive. Because these systems are strictly non-linear, a linearisation is first required to perform stability analysis. First, we make our linear term substitution and subsequent cancelling down, leaving us with the following system (given that the medium acted upon has one spatial dimension):

$$
\begin{aligned}
\xi_t &= D\xi_{xx} - a\delta_{xx} - b\xi, \\
\delta_t &= \delta_{xx} + \xi - \delta.
\end{aligned}
$$

Next we make a substitution for ξ and δ of $\xi(x,t) = \sum_{i=1}^{\infty} \xi^{(t)}(t) cos(\frac{\pi i x}{L})$ and $\delta(x,t) = \sum_{i=1}^{\infty} \delta^{(t)}(t) cos(\frac{\pi i x}{L})$. Having obtained this system, we cancel out the $cos(\frac{\pi i x}{L})$ turning our PDE system into infinitely many ODE systems, for $i \in \mathbb{N}^+$. We also simplify our notation of $\xi^t(t)$ and $\delta^{(t)}(t)$ to $\xi(t)$ and $\delta(t)$, as well as letting $k = \frac{i\pi}{L}$, where k is the wave number of our system:

$$
\dot{\xi} = -Dk^2\xi + ak^2\delta - b\xi, \tag{33}
$$

$$
\dot{\delta} = -k^2\delta + \xi - \delta. \tag{34}
$$

Rewriting this system of equations in matrix form, we obtain the following system. For the next step, let us call the two-by-two matrix below M:

$$\begin{pmatrix} \dot{\xi} \\ \dot{\delta} \end{pmatrix} = - \begin{pmatrix} Dk^2 + b & -ak^2 \\ -1 & k^2 + 1 \end{pmatrix} \begin{pmatrix} \xi \\ \delta \end{pmatrix}.$$

Just as we had done for the homogenous system, we take the Jacobian: more specifically we solve the matrix equation $|M - I\lambda| = 0$, where λ is the eigenvalue and I is the identity matrix. Rewriting this equation to find λ in terms of k^2 we obtain the following:

$$\lambda = \frac{k^2(D+1) + b + 1}{-2} \pm \frac{\sqrt{(Dk^2 + b + k^2 + 1)^2 - 4h(k^2)}}{2}, \tag{35}$$

$$h(k^2) = (Dk^2 + b)(k^2 + 1) - ak^2. \tag{36}$$

From the above equation, we want to obtain a result for λ which is positive for at least one of the roots. Inspecting the term outside of the square root, we note that by conditions derived for the homogenous system, the term will remain negative for all values of k^2.

As such, the square root remains the only term which could cause a root of λ to be negative. Therefore, we require that the square root term must be greater than the term outside the square root for some λ, and in order for that to be the case, we must have that $h(k^2) < 0$. This gives us an inequality in terms of k^2. In order for the inequality to hold given that our parameters are positive, the coefficient of k^2 must be negative, giving us the following condition:

$$k^4 D + k^2(D + b - a) + 1 < 0 \implies a > b + D. \tag{37}$$

In order to progress further, we must find conditions where k^2 is a real, positive number, and for which the inequality holds. In order to find this, we should substitute the inequality with an equation , solve it for k^2, and then translate this result onto our inequality. On that last part, our equation would have to have a "u-shape" because of the k^4 coefficient, and the solution for the inequality would be everything below that line. Therefore, the roots of the equation will form inequalities which will cover 2 separate, unbounded regions, rather than cover one bounded region.
Solving the equation created by substituting the inequality for $= 0$ for k^2 we find:

$$k^2 = \frac{-(D + b - a) \pm \sqrt{(D + b - a)^2 - 4Db}}{2D}.$$

Because the condition we found before was insufficient, we need to find the sufficient condition for our system. This can done by considering the equation

system solved above, specifically with respect to the square root term within it. The square root needs to be positive in order for k^2 to be real, therefore the following inequality can be derived:

$$(D + b - a)^2 - 4Db > 0. \tag{38}$$

We may notice here that the term within the square root bares resemblance to our first distributive condition, 37. As such, we may square root both sides to obtain something resembling that condition, however we much be very mindful of the inequalities here. In addition, we should eliminate the positive square root term as we already know by condition 37 that the $D+b-a$ term is negative. All things considered, we are left with the following inequality, which leads onto our final condition for instability:

$$-2\sqrt{Db} > D + b - a \implies 1 < \frac{a}{DB + 2\sqrt{Db}}. \tag{39}$$

We can also confirm this result by finding the minimum value of $h(k^2)$ for some k^2, and have it be less than 0 as a necessary condition for the distributive system. We find the minimum value of $h(k^2)$ by taking its derivative in k^2 and solving for 0, then substituting our result back into the equation for $h(k^2)$. First we take the derivative of h in terms of k^2 and solve for zero:

$$h'(k^2) = 2k^2D + D + b - a = 0.$$

We rearrange this result to find a minimum value for k^2, namely $k^2 = \frac{a-D-b}{2D}$, and we call this result for k^2 as k^2_{min}. Substituting this into our equation for $h(k^2)$ we obtain the following, after simplification:

$$h({k_{min}}^2) = \frac{4Db - (a - D - b)^2}{4D}.$$

From this equation, considering the inequality $h({k_{min}}^2) < 0$, we note that if we multiply both sides by $4D$ we come to the same inequality as in 38. As such, further derivation will lead us to the same conditions as were attained before.

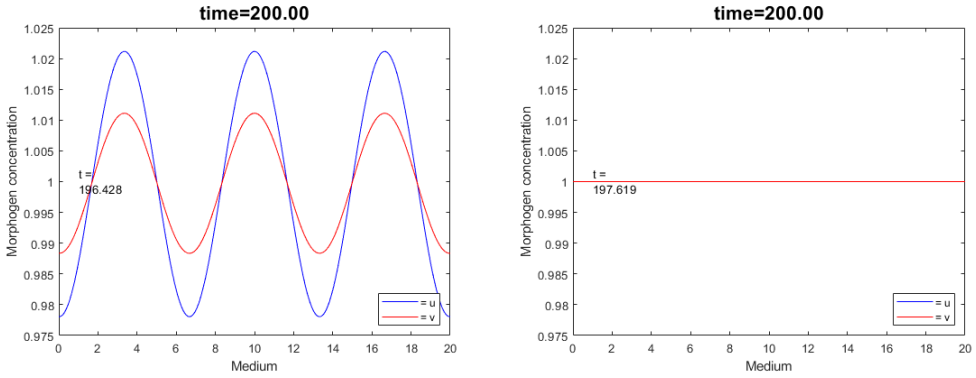

Figure 4: A simulation of morphogen concentrations over time, with the logistic term added. For the first simulation, the conditions for Turing instability are met, therefore the system exhibits characteristic stripes. They are not very large, as the system is prone to collapsing for results with greater wave forms. $a = 4.02, b = 1, D = 2$. For the second simulation, the conditions for instability were not met, and therefore no stripe formation is observed. The y axis was pinned to the same scale as the first image. $a = 1.02, b = 2, D = 5$.

Something to note is that the conditions for stability are barely met. This is due to our term responsible for chemotactic sensitivity, Φ being independent of our u. As the system develops over time, there may occur a spike at which point the value of u, the cell population density, goes negative. Because the logistic term is not equipped to deal with negative values, it can not contain the system within its bounds and our model fails. Specifically, when presented with negative values for u, the concentration of it goes rapidly towards negative infinity with no term being positive. When paused at a certain time for conditions exhibiting this behaviour, this "spiking" may be observed in action. As all the terms in the first equation become negative, this is something we can solve by altering our constant for chemotactic sensitivity, which is what is carried out in the following subsection.

2.3 Non-constant Chemotaxis

The final model considered is a more advanced case of the Keller-Segel model, with non-constant chemotaxis. The purpose of choosing this is to restrict the cell population density from leading to the breakdown of the system due to local negative values being present. The kinetic terms of the system are $k_3 = +\rho A(\delta - A)$, $k_4 = \beta$ and $k_5 = \gamma$, and its chemotactic sensitivity is

$\Phi(u,v) = \alpha A$:

$$A_t = d_u \nabla^2 A - \alpha(\nabla A \nabla B + \nabla^2 B) + \rho A(\delta - A), \tag{40}$$

$$B_t = d_v \nabla^2 B + \beta A - \gamma B. \tag{41}$$

Note that the chemotactic term has been expanded. Our first concern with this system will be to non-dimensionalise it. To do this, we introduce non-dimensionalisation constants and derive further substitutions from them:

$$u = AP, \tau = RtL^{-2}, \qquad u_\tau = \frac{L^2 P}{R} A_t, \qquad \nabla^2 A = \frac{1}{PL^2}\nabla^2 u,$$

$$v = BQ, \chi = xL^{-1}, \qquad v_\tau = \frac{L^2 Q}{R} B_t, \qquad \nabla^2 B = \frac{1}{QL^2}\nabla^2 v,$$

as well as $\nabla(A\nabla B) = \frac{1}{PQL^2}\nabla(u\nabla v)$ .The constants introduced here are P, Q, R, L, allowing us to eliminate up to 4 constants from the original equation system. The non-dimensionalised variables introduced: u, v, χ, tau, represent the cell population density, concentration of positive chemical stimulant, space and time respectively. It should also be noted that ∇ with respect to u and v has also been non-dimensionalised in the above equations. Having constructed adequate non-dimensional substitutions, we substitute them into the equation system to obtain the following:

$$u_\tau = \frac{d_u}{R}\nabla^2 u - \frac{\alpha}{RQ}\nabla(u\nabla v) + \frac{L^2\rho}{R}(\delta - uP^{-1})u,$$

$$v_\tau = \frac{d_v}{R}\nabla^2 B + \frac{\beta L^2 Q}{PR}u - \frac{\gamma L^2}{R}v.$$

Given this system, we are able to now pick our 4 non-dimensionalisation constants to simplify down the system. We may start by making the substitution $R = d_v$ and introducing a diffusion constant $D = \frac{d_u}{d_v}$, which will simplify our diffusion as much as it can be simplified. We may then focus on the kinetics of the system, and make the substitution $L^2 = \frac{d_v}{\gamma}$, which will reduce the coefficient of the degradation of our chemical stimulant to 1. We should also set $P = \delta^{-1}$ as that will allow us to simplify down the bracket in the logistic term. We will then be left with only Q. The substitution chosen is $Q = \frac{d_v}{\gamma\beta\rho}$, which reduces the coefficient of the production of our chemical stimulant to 1. Finally, we group the constant coefficients of the chemotaxis, and the logistic term into one overall non-dimensional variable each: $a = \frac{\alpha\beta\gamma\rho}{d_v^2}$ and $b = \frac{\rho\delta}{\gamma}$. Having obtained a non-dimensional form of this model, shown below, we now move onto analysing it for pattern formation. For convenience, we will replace the τ with t and χ with x from here on.

$$u_t = D\nabla^2 u - a\nabla(u\nabla v) + b(1-u)u, \tag{42}$$

$$v_t = \nabla^2 B + u - v. \tag{43}$$

The above system of equations is the fully non-dimensionalised form of the equation system 40. The constants which remain: D, a, b represent the diffusion rate ratio, the rate of chemotaxis and the strength of the death and growth of the cells kinetic, our logistic term. With non-dimensionalisation complete, we may begin our analysis for pattern formation for the system. The first part of this process will be modelling the system as homogenous and looking for conditions that make the system stable. This means that we will assume that our gradients will be negligible, as such we may, temporarily, assume that out system takes the following form:

$$u_t = b(1-u)u, \tag{44}$$
$$v_t = u - v. \tag{45}$$

We will need to find the fixed points of this system, which we can do by solving the system of equations for u and v when $u_t = v_t = 0$. Doing so will yield us with two fixed points:

$$(u_0, v_0) = (0,0), (1,1).$$

These two fixed points need to be analysed for whether they are stable or unstable. In order to do this, we will linearise 44 and create a Jacobian for the terms within. The matrix will then be solved for its eigenvalues (denoted by the introduced parameter λ), which represent the stability of its solutions.

$$\begin{vmatrix} b(1-2u_0) - \lambda & 0 \\ 1 & -1-\lambda \end{vmatrix} = 0,$$

We may now consider our different cases for u_0, taken from our 2 fixed points:

$$\begin{aligned} u_0 = 0 &: \\ &0 = (b-\lambda)(-1-\lambda), \\ &\lambda = b, -1; \\ u_0 = 1 &: \\ &0 = (b+\lambda)(1+\lambda), \\ &\lambda = -b, -1. \end{aligned}$$

In order for a fixed point to be stable, both values of λ must be less than zero for that fixed point. In the first case, while one fixed point is negative, the other is b. Unless we have a negative logistic term (which is not usually modelled for, and not something we will be modelling for), b must be greater than zero, and as such this fixed point is unstable and may be rejected.

For the second case, both values of λ are less than zero so long as our logistic term is positive, giving us our fixed point: $(u_0, v_0) = (1, 1)$ and our condition for homogeneity: $b > 0$.

We now move onto the distributive case, for which we will need to consider the spatial terms in our system as well. In order to do this, we must linearise our system. This is started off, as before, by introducing linear approximations for our u and v terms, namely ξ and δ, and substituting them into our equations to give the following system:

$$\xi_t = D\xi_{xx} - a\delta_{xx} - b\xi, \tag{46}$$
$$\delta_t = \delta_{xx} + \xi - \delta. \tag{47}$$

As this system has been linearised, we may apply the substitution used before for ξ and δ, namely ξ and δ of $\xi(x,t) = \sum_{i=1}^{\infty} \xi^{(t)}(t) cos(\frac{\pi i x}{L})$ and $\delta(x,t) = \sum_{i=1}^{\infty} \delta^{(t)}(t) cos(\frac{\pi i x}{L})$. From the resulting equations, we cancel out the $cos(\frac{\pi i x}{L})$ terms leaving us with:

$$\dot{\xi^{(t)}} = -Dk^2\xi^{(t)} + ak^2\delta - b\xi, \tag{48}$$
$$\dot{\delta^{(t)}} = -k^2\delta^{(t)} + \xi - \delta, \tag{49}$$

where $(\frac{\pi i}{L})^2 = k^2$. k represents the wave number of the particular ODE under consideration. For convenience, we may drop $\xi^{(t)}$ and $\delta^{(t)}$ in favour of ξ and δ respectively. This completes our preparation for the stability analysis of this distributive model:

$$\dot{\xi} = -Dk^2\xi + ak^2\delta - b\xi, \tag{50}$$
$$\dot{\delta} = -k^2\delta + \xi - \delta. \tag{51}$$

For the stability analysis, we are looking for solutions where there exists a value for λ that is greater than zero. This may also be found by obtaining the Jacobian matrix of our system, and then checking its trace and determinant. If the trace of the matrix is positive, then there has to be at least one positive eigenvalue regardless of the determinant. However, if the trace is negative, then the determinant of the matrix must be greater than zero for there to exist a positive solution for the eigenvalue λ.

$$\begin{pmatrix} -Dk^2 - b & ak^2 \\ 1 & -k^2 - 1 \end{pmatrix}. \tag{52}$$

The trace of 52 is clearly negative, therefore we must find the determinant

for positive values, which will give us our condition for Turing instability.

$$0 < -ak^2 + Dk^2 + bk^2 + Dk^4 + b, \tag{53}$$

$$< k^4 + k^2(D + b - a) + b, \tag{54}$$

$$k_+^2 > \frac{-(D + b - a) + \sqrt{(D + b - a)^2 - 4Db}}{2}, \tag{55}$$

as the negative root moves away. For $k^2 > 0$ we have as a necessary condition that:

$$D + b - a < 0, \tag{56}$$

as well as the sufficient condition that:

$$(D + b - a)^2 > 4Db. \tag{57}$$

Having found the conditions for pattern formation, we may now move onto simulation. Attempting to use the scheme used in previous figures, we find that it is inadequate for modelling this chemotactic model. Though this will be covered in more detail in the next section, the reason for this occurring is due to the presence of spatial derivatives in the first order, which under the numerical modelling used for the previous two sections implies three possible methods to be used, all of them inadequate. Instead, a different numerical model was obtained, for which simulations were ran under conditions specified.

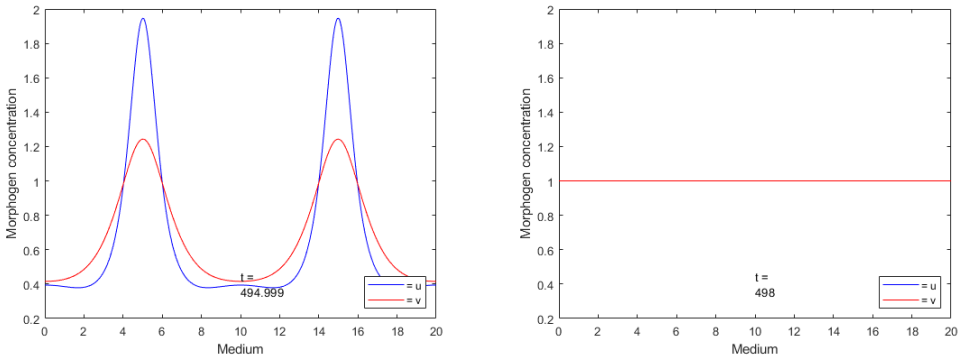

Figure 5: A simulation of morphogen concentrations over time, with the logistic term added. For the first simulation, the conditions for Turing instability are met, therefore the system exhibits characteristic stripes. $a = 4.02, b = 0.1, D = 2$. For the second simulation, the conditions for instability were not met, and therefore no stripe formation is observed. The y axis was pinned to the same scale as the first image. $a = 1.02, b = 2, D = 5$

.

The simulations found that when the conditions of stability and instability were met, there were indeed patterns exhibited on the medium by the morphogens. Furthermore, when pattern conditions were not met, these patterns disappeared. Unlike the models in sections 2.1 and 2.2, there were no problems noticed with respect to unexpected large growth of concentrations over time, nor of the exhibitance of negative concentrations, which makes the model suitable for the simulations of basic chemotactic systems.

Conclusion

Analysing the Keller-Segel model system of equations as described in section 1.2 and in [12], we were able to obtain non-dimensionalised models for three specific cases, as well as derive their conditions for pattern formation and demonstrate that they do indeed hold under appricable numerical simulations. In addition, covered were the limitations of variants of this model where chemotaxis is constant as well as variants without a term controlling the growth and decay of one of the system's morphogens. Specifically, lacking a growth and decay term leads to patterns which may constantly grow in amplitude as well as take on negative values.

Addressing this, however, without having a chemotactic term dependent on morphogen concentrations can lead to problems, demonstrated here by a logistic solution causing negative concentrations to lead to the model breaking down. Eventually, stable pattern formation results were derived for a model exhibiting non-constant chemotaxis which dealt with the aforementioned problem. Stable pattern formation conditions were obtained under a similar process followed in [13], where stable points and conditions for stability were found for a model not exhibiting chemotaxis or diffusion. These conditions were then used in the stability analysis of the full model, with functioning chemotaxis and diffusion, for unstable results. For the most basic model, with no logistic term and constant chemotaxis, the condition found was that $\frac{a}{D(k^2+1)} > 1$, for a family of fixed points where $u_0 = v_0$.Overall, however, a non-dimensional system and conditions were found for stable pattern formation with realistic cell population densities, as well as the conditions for the existence of such a system. Further possible work in this area may include the derrivation of conditions for pattern formation as described in [20] of the general Keller-Segel model, or for more modes of non-constant chemotaxis.

3 Numerical Algorithms

Introduction

In this section we will discuss the methods approached for simulating the models employed for chemotaxis in the previous section, as well as discussing the problems encountered in simulations and reasons for using certain schemes, as well as their utility in obtaining solutions for pattern formation problems. We will outlay the reason for implementation of numerical algorithms as a tool for solving non-linear problems, as well as how they are constructed from analytical problems. We will also describe the stability of our solutions, the cases for which it does not suffice, as well as alternate schemes which may remedy these issues. In terms of the schemes described, of particular interest to us will be the Forward-Time Centred-Space scheme, as well as the Lax-Friedrichs scheme for advection-containing problems, namely that presented in section 2.3 with non-constant chemotaxis. Indeed, the advection arises from this, as the chemotactic term is no longer $a\nabla^2(v)$, but $a\nabla(u \cdot \nabla v)$, expanding out to $a\nabla^2 v + a\nabla u \nabla v$ where the medium is in one spatial dimension.

Numerical methods are a powerful tool in the analysis of partial differential equation systems. Because of the nature of partial differential systems, obtaining an exact analytical solution for the system presented can be difficult if not impossible. One factor which complicates this is non-linearity of equations, that is systems which can not be rewritten purely in terms of a linear combination of unknown variables found in them. For linear systems, numerical methods can be avoided by performing row reduction, for instance, which can be performed by computers with relative ease. However, this avenue is often unavailable in the analysis of dynamical systems with which we are concerned. In-fact, the bulk of systems appearing naturally are non-linear [7], including all systems which experience Turing Instability [15]. As such, numerical methods were utilised in obtaining approximate simulations of the systems concerned.

3.1 Introductory example: Euler & Stability

In order to apply numerical methods to a system of equations, be they ordinary or partial, the differential equations must first be turned into difference equations. In order to do this, sufficient initial (or boundary in the event of partial equations) conditions of the system must be known to satisfy the

numerical model being employed.

For instance, let us consider one of the oldest explicit numerical methods in existence, the forward Euler method on a 1st order ordinary differential equation. While this method for solving ordinary differential equations can be applied for n-th order differential equations with ease, this is not necessary for the demonstration. In addition, while being an ordinary differential equation method, its operation is still useful for considering the workings of the partial differential methods that were applied for the numerical simulations of chemotaxis, as well as being a good entry point for analysis of stability and stiffness. Let us therefore define such a function in differential terms, namely:

$$\begin{aligned}\frac{df(t)}{dt} =& F(t, f(t)),\\ f(t_0) =& f_0,\end{aligned}$$

and assume that $f(t)$ is continuous and its derivative finite. In order to approximate a numerical solution for this function, we are going to employ a discretisation grid with evenly spaced argument values, that is to say we will take time at the initial condition t_0 and have further time inputs be of the form $t_i = t_0 + i\Delta t$, where $i \in \mathbb{N}_+$, with Δt representing the size of the time step. Having done this, we may now rewrite our differential equation as a difference equation, represented below:

$$\begin{aligned}\frac{df(t_i)}{dt} =& F(t_i, f(t_i)),\\ f(t_0) =& f_0.\end{aligned}$$

In essence, the above equation allows us to obtain the gradient at a particular point, given its f and t coordinates. As our initial conditions specify both of those values at $i = 0$, we can easily obtain the gradient at the original point.

Now we move onto obtaining approximations for further points from the initial conditions. Since t_{i+1} is given by adding the step size onto t_i, and we can derive the gradient at the following point from t_{i+1} and $f(t_{i+1})$ the only value that remains to be found is $f(t_{i+1})$, which we will call f_{i+1} for brevity. The forward-step Euler method relies on using the following numerical approximation

$$\frac{df_i}{dt_i} \approx \frac{f_{i+1} - f_i}{\Delta t}, \tag{58}$$

to arrive at an estimate for f_{i+1} from already known variables. We call this method "forward Euler" because it uses "forward difference", or values dependent (exclusively except for i) on $i+1$ rather than $i-1$ to obtain an estimation for $\frac{df_i}{dt_i}$. We may rewrite the above equation to give us an estimate solution for f_{i+1}:

$$f_{i+1} \approx \Delta t \frac{df_i}{dt} + f_i.$$

Combined with our solution for $\frac{df_i}{dt}$, we have derived a numerical algorithm for obtaining progressive estimates for f_i as time progresses:

$$f_{i+1} \approx \Delta t F(t_i, f(t_i)) + f_i,$$

where t_0 and f_0 are known by initial conditions. From this, we can rewrite our function to denote that it has been discretised, allowing us to drop the approximate for an equals and clearing up notation in stability analysis:

$$\bar{f}_{i+1} = \Delta t F(t_i, f(t_i)) + \bar{f}_i, \tag{59}$$

where $\bar{f}_0 = f_0$. This model is a relatively simple one, which does come with its drawbacks. First, we should consider that it is a forward system, or "upwind" as it may also be called. This means that only values that are preceding $\bar{f}_{i+1}$ are used to approximate it ($\bar{f}_i$, namely). While this makes intuitive sense for schemes approximating time, it nonetheless introduces a forward-bias into the system, which introduces more instability and error into the system that could be had under a central difference scheme. Indeed, this was a problem encountered further on in the modelling of chemotactic partial differential equations, albeit in space rather than time.

Another key problem of note is the discretisation error of the system. Let us first consider the forward finite difference approximation of equation 59, provided in [16] :

$$\frac{df(t)}{dt}\Big|_{t=t_i} = \frac{d^2 f(t)}{dt^2}\Big|_{t=T} \frac{\Delta t}{2} + \frac{f_{i+1} - f_i}{\Delta t},$$

where T is a time within the range of times simulated, that is $T = t_i, i \in \mathbb{N}_0$. Our discretisation error is found by subtracting from this equation the approximation for $\frac{df}{dt}\Big|_{t=t_i}$ that was used to obtain our Euler method, namely 58, with t_i being set as t_0:

$$\begin{aligned} \left|\bar{f}_1 - f_1\right| =& \frac{d^2 f(t)}{dt^2}\Big|_{t=0} \frac{\Delta t}{2} + \frac{f_{i+1} - f_i}{\Delta t} - \frac{f_{i+1} - f_i}{\Delta t}, \\ \left|\bar{f}_1 - f_1\right| \leq& M_2 \frac{\Delta t}{2}, \end{aligned}$$

where $M_2 \geq \frac{d^2 f(t)}{dt^2}\Big|_{t=0}$. The term on the left hand side of the above equation represents the local error of the system. What is apparent is that because M_2 is independent of the time step Δt, the local error can be dependently reduced by applying a sufficiently small step size.

Finally, the Euler method is an explicit method. Explicit methods have the advantage of being relatively light in terms of required computing power and being easier to set up than their implicit counterparts. However, this comes at the cost of stability being more conditional, based on the equation being modelled as well as the time step size. In effect, explicit methods have a limited stability region, which can be derived by various methods.

For the explicit Euler method, we will utilise the test function method. This method applies a test function $\frac{df}{dt} = \lambda t f$ under the explicit Euler method to obtain a function $\Phi(\Delta t \lambda)$ such that $f_{i+1} = \Phi(\Delta t \lambda) f_i$. In order for the method to be stable, the function Φ must have an absolute magnitude less than 1. For our explicit Euler method:

$$\begin{aligned} f_{i+1} =& \Delta t F(t_i, f_i) + f_i, \\ =& \Delta t(\lambda f_i) + f_i, \\ =& (\Delta t \lambda + 1) f_i, \end{aligned}$$

with $\Phi = \Delta t \lambda + 1$, which implies that the region of stability for the explicit Euler method is a unit circle centred around $(-1, 0)$ in the complex plane. With this it becomes apparent how explicit methods such as the forward Euler scheme used here are prone to suffer from stiffness and instability of solutions if these factors are not carefully controlled for.

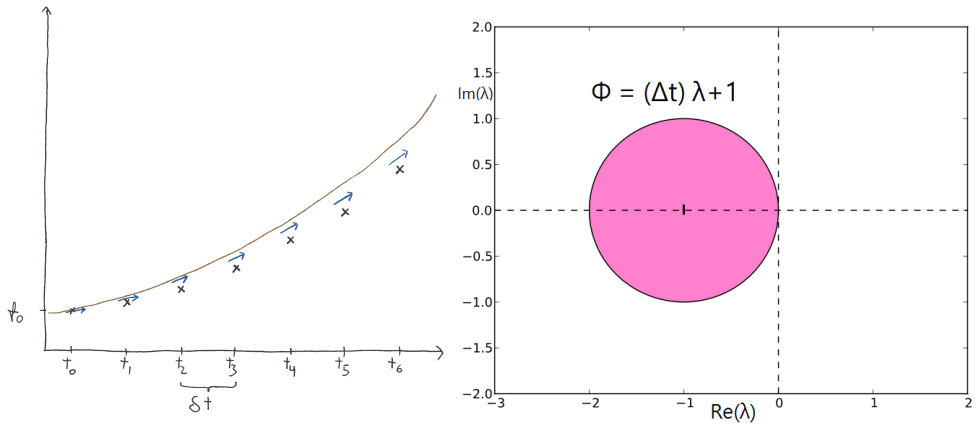

Figure 6: On the left: an illustration of an example of the forward-Euler method. The brown line represents some function which is being approximated, while the black crosses represent the approximate solutions for f at the given time. Note that these are based on the gradient of the line as approximated at the preceding point, leading to an increase in error over time, especially at larger step sizes (that is to say, larger Δt.). This is because as Δt tends to zero, the numerical solution tends to the actual solution as the system is continuous . The gradient at the point is represented by the blue arrow at each point. The step size, Δt is also shown. On the right: an illustration of the stability diagram for an explicit Euler method. As previously derived, the stability region for this method is bound within a unit circle about the point $(-1, 0)$, the equation of which is given on the diagram, on the complex plane. The vertical axis is imaginary.

3.2 PDEs: Forward Time Central Space scheme

Having introduced the principles of numerical schemes as they pertain to ordinary differential equations and the limitations they come upon, we now move onto partial differential equations and methods for their simulation and stability analysis. In-fact, there is some overlap between the methods and problems encountered for partial differential equations and ordinary differential equations. However, in partial differential equations the matter is complicated by the addition of a variable for space, as well as the compounding of error and instability between the two independent variables. In the following subsection we will discuss a partial differential scheme which follows fairly smoothly on from the forward time explicit Euler scheme.

The first partial differential scheme with which we are concerned is the Forward-Time Centred-Space scheme. As the name suggests, the scheme

essentially relies on the spatial components being approximated "centrally", that is to say from both the left and the right , while approximating the change in time as it evolves forwards (akin to the Euler method for ordinary differential equations). Being a finite difference method explicit in time, it is relatively light in terms of computations and well suited for solving parabolic partial differential equations.

When simulating a partial differential equation system, it is important to know what kind of system it is, that is whether it is hyperbolic, parabolic or elliptic. The reason for this is that different numerical methods are applicable to different types of systems. In order to ascertain whether the system is parabolic, hyperbolic or elliptic, the equation on the left hand side is used, where the equation being tested is of the form displayed on the right:

$$\begin{aligned}\Delta =& B^2 - AC, \text{for:}\\ G =& Au_{xx} + Bu_{tx} + Cu_{tt} + Du_x + Eu_t + Fu,\end{aligned}$$

where Δ being positive, zero or negative corresponds to the equations being hyperbolic, parabolic or elliptic respectively. In order to use the forward-time centred-space scheme, the condition $B^2 - AC = 0$ must be met, that is the equation must be parabolic.Because the morphogens in the system are not dependent on $\frac{\partial^2}{\partial x \partial t}$ or $\frac{\partial^2}{\partial t \partial t}$, the parabolic condition is always satisfied.

Just as we had done for the Euler method, we will also draw a discretisation grid. The points on this grid will be evenly spaced apart in space and in time, but not necessarily the same spacing between the two, that is to say the grid is made up of congruent rectangles.

Looking at the problem as it is presented on a discretisation grid, we can think of the approximation as taking place in two parts. The first part is the approximation of the spatial components, done through a central difference scheme as will be elaborated on further, and the second part is their utilisation in approximating a forward time scheme, in a not too dissimilar way to the Euler discussed in the previous subsection. As such, for now it may be useful to consider the two parts separately, and then once the scheme is laid out to bring them together and analyse for stability and any drawbacks, as well as to demonstrate its applications as used in modelling constant chemotaxis.

Temporal component
We will start off with the temporal component. As previously stated, the

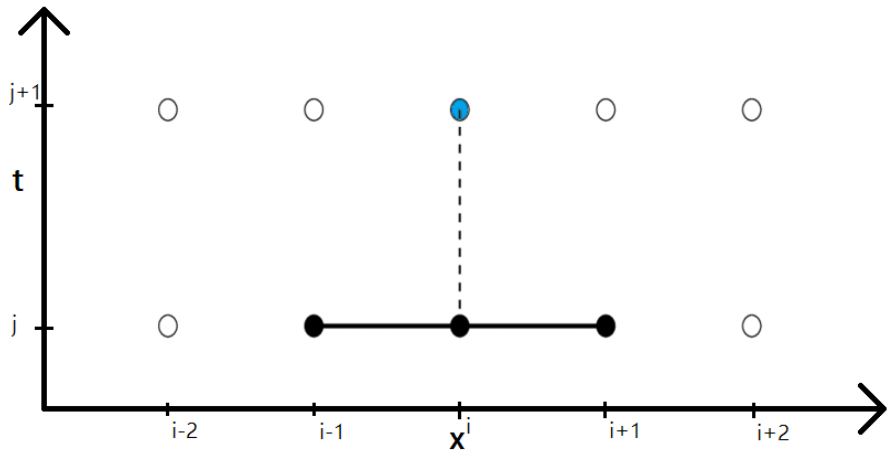

Figure 7: An illustration of a Forward-Time Centred Space grid. The horizontal represents the spatial component, or the medium upon which the morphogens act, while the vertical is a stand in for forward time. The black dots represent the three points ($x = i - 1, i, i + 1$ at $t = j$) whose values are needed to generate the fourth point ($x = i, t = j + 1$) , represented in blue.

time component can be thought of as being similar to the explicit Euler method which was solved for as an example. Consider a partial differential system with one equation for now. This system can easily be written as

$$u_t = F(x, t, u, u_x, u_{xx}, ...),$$

where u_x is included, but later on it will be shown that problems exist for all odd-numbered derivatives in x. Grouping all of the t-dependent terms on the left, seperate from the space-dependent terms allows us to put their analysis to one side temporarily and allows us to focus on the left hand side. Discretising this system, we obtain the following system by making a forward difference substitution for u_t:

$$\frac{u_i^{j+1} - u_i^j}{\Delta t} = F(x, t, u, u_x, u_{xx}, ...)_i^j,$$

where u_i^j refers to the value of u at $x = x_i, t = t_j$. For this system, like with the explicit forward euler method, we multiply both sides by Δt, as well as move u_i^j to the right hand side to obtain an at this time sufficient result for u_i^{j+1} in terms of u-s at $t = t_j$.

$$u_i^{j+1} = u_i^j + (\Delta t) F(x, t, u, u_x, u_{xx}, ...)_i^j. \tag{60}$$

We can therefore use this result to calculate the numerical scheme, given the function $F(x, t, u, u_x, u_{xx}, ...)$, after it has been discretised. Because this holds for different functions of F, we may use this result for different spatial components, so long as they fit under the forward time central space scheme. In the following part, we will be relying on our result for just that end, as we will consider different functions for $F(x, t, u, u_x, u_{xx}, ...)$, as well as expanding our result to systems of two equations.

3.2.1 Spatial component and result: Heat equation example

Here, we are concerned with finding a numerical approximation to the spatial components of the problem, given a certain time. To this end, we need to find an appropriate, centrally fixed solution. We will start off by considering a very simple example: the heat equation with only one spatial dimension for demonstration purposes of methods employed in deriving the system:

$$u_t = du_{xx},$$

where k is the diffusion coefficient, and the boundary conditions of the heat equation are given by:

$$0 < x < L, \text{where L is the length of the medium acted upon.}$$

In order to obtain an approximation for the left hand side without changing in time, we can think of our term on the right hand side as a function which we are trying to approximate in space only, for a given time j. As such, we can express our equation alike to how we had done previously for the temporal component:

$$u_t = F(x, t, u, u_{xx}) = ku_{xx},$$

which we can discretise to yield (given that j is already given by the temporal part):

$$F_i = d(u_{xx})_i.$$

Because this method relies on the central difference scheme to operate, the only substitutions for u and its derivatives that should be used are ones which are "balanced" between $i + n$ terms and $i - n$ terms, where n is a positive integer. In this example, the only substitution that needs to be made is for $(u_{xx})_i$ which can be done by finding the difference between the forward and

backward difference:

$$\begin{aligned}(u_x)_i =& \frac{u_{i+1} - u_i}{\Delta x},\\ (u_x)_{i-1} =& \frac{u_i - u_{i-1}}{\Delta x},\\ (u_{xx})_i =& \frac{(u_x)_i - (u_x)_{i-1}}{\Delta x^2},\\ =& \frac{u_{i+1} + u_{i-1} - 2u_i}{\Delta x^2},\end{aligned}$$

where Δx is the space step size. We may then substitute to give us the following for F_i:

$$F_i = d\frac{u_{i+1} + u_{i-1} - 2u_i}{\Delta x^2}. \tag{61}$$

Having obtained a numerical approximation for the spatial components of the model at a given time j, we may now move onto bringing them together with the temporal components to form the forward time central space scheme by substitution. Substituting 61 into 3.2.2, we obtain the following equation:

$$u_i^{j+1} = u_i^j + (\Delta t)d\frac{u_{i+1}^j + u_{i-1}^j - 2u_i^j}{\Delta x^2},$$

which we can rewrite such that the "step terms" Δt and Δx are grouped together to give us the FTCS scheme for the heat equation:

$$u_i^{j+1} = u_i^j + d\frac{\Delta t}{\Delta x^2}(u_{i+1}^j + u_{i-1}^j - 2u_i^j). \tag{62}$$

Von Neumann Stability Analysis

Now that a scheme has been obtained, we turn to analysing its stability. Because the scheme we are dealing with is one for a partial differential equation, different method are utilised for their stability analysis. The method which we will be employing is the von Neumann stability analysis, also called Fourier stability analysis.

The von Neumann method of stability analysis relies upon, like the method for ordinary differential equations explored in the previous sections, upon finding the ratio in error between the "next step" and the current step. However, because partial differential equations have at least two lines along which steps progress, further work needs to be done to prepare the system for such analysis. Specifically, a Fourier series is generated for the error term

which separates the temporal and spatial components, which is then made to cancel down in the analysis for finding the ratio between the next time step and the current time step Fourier term. While the Fourier methods play a part in obtaining the substitution, these methods have been covered in section 2 for the linearisation fo the distributive system, and as such will be only briefly covered.

Before the von Neumann analysis is started, it is important to distinguish clearly between the exact solution of the problem and the numerical approximate solution generated. This wasn't as much of a problem before due to u (without superscript and subscript notation) denoting the prior while u_i^j denoted the latter, however to proceed with this method analytical solutions for u need to be presented on the discretisation grid co-ordinate system. As such, henceforth the numerical solution for the problem shall be denoted by M_i^j and the analytical by u_i^j notation, on the same bounds as before.

Having established a clear notation, we can now define a term for the round-off error of the system:

$$\eta_i^j = M_i^j - u_i^j.$$

Having defined our round off error we may proceed to substitute it into equation 62. We may substitute the error term because both of the terms constituting it, M_i^j and u_i^j are solutions to the original equation.

$$\eta_i^{j+1} = \eta_i^j + d\frac{\Delta t}{\Delta x^2}(\eta_{i+1}^j + \eta_{i-1}^j - 2\eta_i^j). \tag{63}$$

At this stage, we proceed by making a Fourier series substitution for η. This results in us obtaining the substitution found in [14], where $C^k(t)$ corresponds to the terms dependent on time, and k is the wave number of the Fourier substitution, for $k \in \mathbb{Z}$:

$$\eta_i^j = C_k(t)e^{kx\sqrt{-1}}. \tag{64}$$

The above relation can then be used to generate appropriate substitutions for each η, namely:

$$\eta_i^{j+1} = C_k(t + \Delta t)e^{kx\sqrt{-1}},$$
$$\eta_{i+1}^{j} = C_k(t)e^{k(x+\Delta x)\sqrt{-1}},$$
$$\eta_{i-1}^{j} = C_k(t)e^{k(x-\Delta x)\sqrt{-1}}.$$

At this stage we are nearing the construction of our stability criterion. The stability criterion is defined as a ratio between the value of η at the future time step and it at the current time step. For a scheme to remain stable, the magnitude of this ratio has to remain below one for all terms within it as a necessary and sufficient condition. We can derive this ratio in terms of our Fourier results by first solving for the ratio in terms of C_k, and then rewriting 63 to find the ratio.
Let us start by deriving the stability criterion, which we will call G:

$$G = \frac{\eta_i^{j+1}}{\eta_i^{j}} = \frac{C_k(t + \Delta t)e^{kx\sqrt{-1}}}{C_k(t)e^{kx\sqrt{-1}}} = \frac{C_k(t + \Delta t)}{C_k(t)}.$$

From this result, we can establish that in order for our system 63 with substitutions for η derived from 64 to give us the ratio, we must solve it for $\frac{C_k(t+\Delta t)}{C_k(t)}$. We start off by writing 63 with appropriate substitutions derived from 64:

$$\begin{aligned} C_k(t + \Delta t)e^{kx\sqrt{-1}} =& C_k(t)e^{kx\sqrt{-1}} \\ &+ dC_k(t)\frac{\Delta t}{\Delta x^2}(e^{k(x+\Delta x)\sqrt{-1}} + e^{k(x-\Delta x)\sqrt{-1}} - 2e^{kx\sqrt{-1}}). \end{aligned}$$

We can now divide both sides by $C_k(t)e^{kx\sqrt{-1}}$ to obtain the stability criterion:

$$\frac{C_k(t + \Delta t)}{C_k(t)} = 1 + d\frac{\Delta t}{\Delta x^2}(e^{k\Delta x\sqrt{-1}} + e^{-k\Delta x\sqrt{-1}} - 2). \tag{65}$$

While this solution is technically correct, it can be simplified down further before it is brought into an inequality. First off, the exponential identity for cosine($2cos\theta = e^{i\theta} + e^{-i\theta}$) can be used to eliminate the exponential terms and consolidate them into a single function. In addition, the trigonometric identity ($cos\theta - 1 = -2sin^2(\theta \div 2)$) can be used to bring all the partial differential terms together into a single expression:

$$G = 1 - d\frac{\Delta t}{\Delta x^2}\left(4sin^2\frac{k\Delta x}{2}\right). \tag{66}$$

Having obtained a relatively simplified expression, we may now solve the inequality problem of $|G| \leq 1 \forall k$. We can start off by noting that $\sin^2\theta$ is strictly positive, therefore we may discount the upper bound and solve for $G \geq -1$ only. Rearranging we arrive at::

$$\frac{1}{2} \geq d\frac{\Delta t}{\Delta x^2}\left(sin^2\frac{k\Delta x}{2}\right).$$

Because the size of sin^2 ranges between zero and one inclusively, and it being equal to 1 puts the greatest constraint on the stability criterion (which as aforementioned, needs to hold for all values of k), we let $sin^2\frac{k\Delta x}{2} = 1$. This gives us the most simplified form of our stability criterion, namely:

$$\frac{1}{2} \geq d\frac{\Delta t}{\Delta x^2}, \tag{67}$$

that is, the ratio between the step size of time and the step size of space must not exceed $\frac{1}{2d}$. In summary therefore, the forward time central space scheme is stable for the heat equation given sufficiently small step sizes for the condition in 67 to be met. This result demonstrates that diffusion-driven systems are stable under the forward time central space scheme if there are no other terms complicating the matter and the conditions are met.

In the following paragraph, we will be considering the Keller-Segel model without advection terms, that is to say containing only 2nd order differentiations besides non-differentiated terms. Unlike the heat equation problem however, the Keller-Segel model is a system of two equations with a chemotactic term, albeit one which is under constant chemotaxis.

3.2.2 Spatial component and result: Keller-Segel

Consider our non-dimensionalised equation system from section 2.2, the logistic-termed constant chemotaxis system 28. As mentioned in previous sections, the terms a, b, D correspond to the non-dimensionalised chemotactic term, the logistic growth/decay term and the diffusion rate ratio respectively. This system is given by:

$$\begin{aligned} u_t &= D\nabla^2 u - a\nabla^2 v + bu(1-u), \\ v_t &= \nabla^2 v + u - v, \end{aligned}$$

under zero flux boundary conditions acting on the medium, $x \in [0, L]$. It is apparent from observing the system that our numerics will be concerned

with only 2nd order derivatives in space, as well as points for which solutions already exist. This is good news for us, as will be explained in more detail later, because we will only have to approximate a 2nd order derivative with a relatively simple to implement central scheme. In addition, it should be noted, that our equation in section 2.1 differs from the one we are concerned with here only in that it is missing the logistic term. As such, everything covered here will apply equally to it for the purposes of modelling the numerical scheme, as a substitution of $b = 0$ can be made to bring the system to the form expressed in section 2.1.

As we have already calculated an appropriate scheme for the temporal component, we can start off by focusing immediately on the spatial scheme. In order for the system to be discretised, we will employ the same numerical approximations for u and its derivatives as we had done previously for the heat equation. However, unlike the heat equation for which they were derived, the Keller-Segel model is a system of two equations. As such, these same discretisations and difference approximations are made for the other independent variable, v:

$$v(x,t) \approx v_i^j, \qquad v_{xx}(x,t) \approx \frac{v_{i+1}^j + v_{i-1}^j - 2v_i^j}{(\Delta x)^2}.$$

The Keller-Segel systems analysed all have only one spatial dimension, therefore we can now substitute these approximations into the "constant chemotactic" Keller-Segel equation to give us the following scheme for numerical approximation:

$$F_i^j = \frac{D}{(\Delta x)^2}(u_{i+1}^j + u_{i-1}^j - 2u_i^j) - \frac{a}{(\Delta x)^2}(v_{i+1}^j + v_{i-1}^j - 2v_i^j) + bu_i^j(1 - u_i^j),$$
$$G_i^j = \frac{1}{(\Delta x)^2}(v_{i+1}^j + v_{i-1}^j - 2v_i^j) + u_i^j - v_i^j.$$

This is, of course, incomplete, as the temporal components need to be added into the scheme. In order to do this, the result derived previously in equation may be used, expanded to accommodate a system of two equations:

$$u_i^{j+1} = u_i^j + (\Delta t)F(x,t,u,u_x,u_{xx},...)_i^j,$$
$$v_i^{j+1} = v_i^j + (\Delta t)G(x,t,v,v_x,v_{xx},...)_i^j,$$

into which we may substitute the spatial components scheme as obtained

above:

$$u_i^{j+1} = u_i^j + D\frac{\Delta t}{(\Delta x)^2}(u_{i+1}^j + u_{i-1}^j - 2u_i^j) \tag{68}$$

$$- a\frac{\Delta t}{(\Delta x)^2}(v_{i+1}^j + v_{i-1}^j - 2v_i^j) + b\Delta t u_i^j(1 - u_i^j), \tag{69}$$

$$v_i^{j+1} = v_i^j + \frac{\Delta t}{(\Delta x)^2}(v_{i+1}^j + v_{i-1}^j - 2v_i^j) + \Delta t(u_i^j - v_i^j), \tag{70}$$

which gives us the numerical scheme used for modelling systems in section 2.1 and 2.2. This scheme remains stable on the condition that the ratio of the time step and space step remain small enough during the simulations.

In order to run simulations of this code, MATLAB was used, with some additional steps being taken. Firstly, constant initial conditions were given for u and v at $t = 0$ or $i = 0$ except for a small perturbation about the centre of the medium. The specific values in code were $u_i^0, v_i^0 = 0.5$ except for a grouping of eleven coordinates for u_i^0 and v_i^0 each, centred around the midpoint of the medium, $L \div 2$.

In addition to this, the code simulated the development of the model through time by giving a snapshot of the morphogen concentrations on the medium, at set time intervals. Finally, the values for the space step size and the time step size used were $\Delta = 0.05$ and $\Delta = 1 \div 42000$, giving a step ratio of $1 : 210$, which should be sufficiently small that the stability criterion is met for diffusion.

In summary, the forward time central space scheme is well suited to these two problems exhibiting constant chemotaxis, however the scheme has thus far only been applied to such problems in this disscertation. In section 2.2, it was observed that constant chemotaxis was causing problems due to the then newly introduced logistic term. As a result, an advection term was instead added, and the forward time central space scheme we have thus far used came upon some problems which will be further discussed in the next section.

3.2.3 Limitations: Upwind and Downwind Accuracy

The introduction of non-constant chemotaxis presents a problem for the forward time central space scheme that it is not too well equipped to deal with. To understand why, it would be good to first cover upwind and downwind

schemes as they arise for first order and second order partial differential equations.

When constructing a difference equation to approximate the numerical result of a differential equation, conventionally there are two ways to go about this. Consider a first order differential equation. We are trying to obtain a value for $(u_x)_i^j$ by taking the difference between two points where the time coordinate remains the same . The first method, upwind, would go about this by taking the point u_i^j as well as the next point over to the right, u_{i+1}^j, and dividing them by the space step term Δt. The second method, downwind, would instead take the next point over to the left instead, u_{i-1}^j.

There also exist other methods, such as the "central difference", which involves taking the points u_{i-1}^j and u_{i+1}^j and dividing them by twice the space step. All of these approaches have their downsides: the upwind and downwind schemes only consider points on the medium to the right or the left of the gradient coordinate, which interferes with the pattern formation process that is being modelled; the central difference scheme on the other hand has a much larger effective step size which reduces stability, and will later be found to be conditionally unstable.

$$(u_x)_i^j = \frac{u_{i+1}^j - u_i^j}{\Delta x}, \quad (u_x)_i^j = \frac{u_i^j - u_{i-1}^j}{\Delta x}, \quad (u_x)_i^j = \frac{u_{i+1}^j - u_{i-1}^j}{2\Delta x}. \tag{71}$$

The equations above represent upwind, downwind and central difference respectively. The problems which arise from the upwind and downwind schemes can be better visualised on the discretisation grid, where it becomes apparent that the upwind and downwind schemes are able to utilise less reference points, especially for values of x approaching L for the upwind scheme, and values of x approaching 0 on the downwind scheme.

Demonstration of issues with advection for the upwind space scheme:

To demonstrate the issues which arise from utilising an upwind or downwind scheme for the spatial component of the numerical model, we will use the upwind scheme to generate simulations for the non-constant chemotactic model used in section 2.3. The non-dimensionalised model used in that subsection (equation 42) had the form:

$$\begin{aligned} u_t &= D\nabla^2 u - a\nabla(u\nabla v) + b(1-u)u, \\ v_t &= \nabla^2 v + u - v. \end{aligned}$$

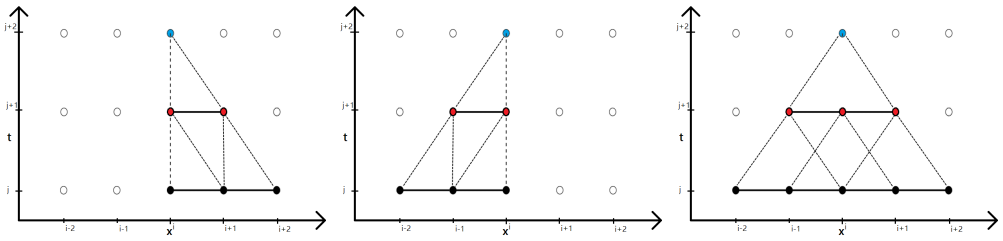

Figure 8: Discretisation grids for first order difference equations. From left to right: upwind, downwind, central difference. Dotted lines represent which points alower down in time are required to generate an approximation for the corresponding point gradient. Black points are used to generate the gradients at the red points, while the red points are used to generate the gradients at the blue. Note that upwind and downwind approximations rely on less points in general as the scheme evolves through time as compared to the central difference scheme, and would only be able to interact with one medium boundary.

First off, we should recall that the system operates in one spatial dimension. As such, the advection term can be easily differentiated to give the following system to be simulated:

$$\begin{aligned} u_t &= Du_{xx} - a(u_x v_x + u v_{xx}) + b(1-u)u, \\ v_t &= v_{xx} + u - v. \end{aligned}$$

As the numerical model for the system without advection was derived previously in this section, we will use that equation system with the upwind scheme defined in 71 to obtain a numerical model for the system with advection, given by:

$$\begin{aligned} u_i^{j+1} =& u_i^j + D\frac{\Delta t}{(\Delta x)^2}(u_{i+1}^j + u_{i-1}^j - 2u_i^j), \\ & - a\frac{\Delta t}{(\Delta x)^2}((u_{i+1}^j - u_i^j)(v_{i+1}^j - v_i^j) + u_i^j(v_{i+1}^j + v_{i-1}^j - 2v_i^j)) + b\Delta t u_i^j(1-u_i^j), \\ v_i^{j+1} =& v_i^j + \frac{\Delta t}{(\Delta x)^2}(v_{i+1}^j + v_{i-1}^j - 2v_i^j) + \Delta t(u_i^j - v_i^j), \end{aligned}$$

using the central scheme for second order terms. Based on our calculations and numerical results in section 2, we should expect to see stable and symmetric patterns form along the length of the medium. However, running

simulations of this code for the stable coefficients as used in figure 5 on page 25 (that is, $a = 4.02$, $b = 0.1$, $D = 2$) we find that the simulations behave quite differently to what we would expect.

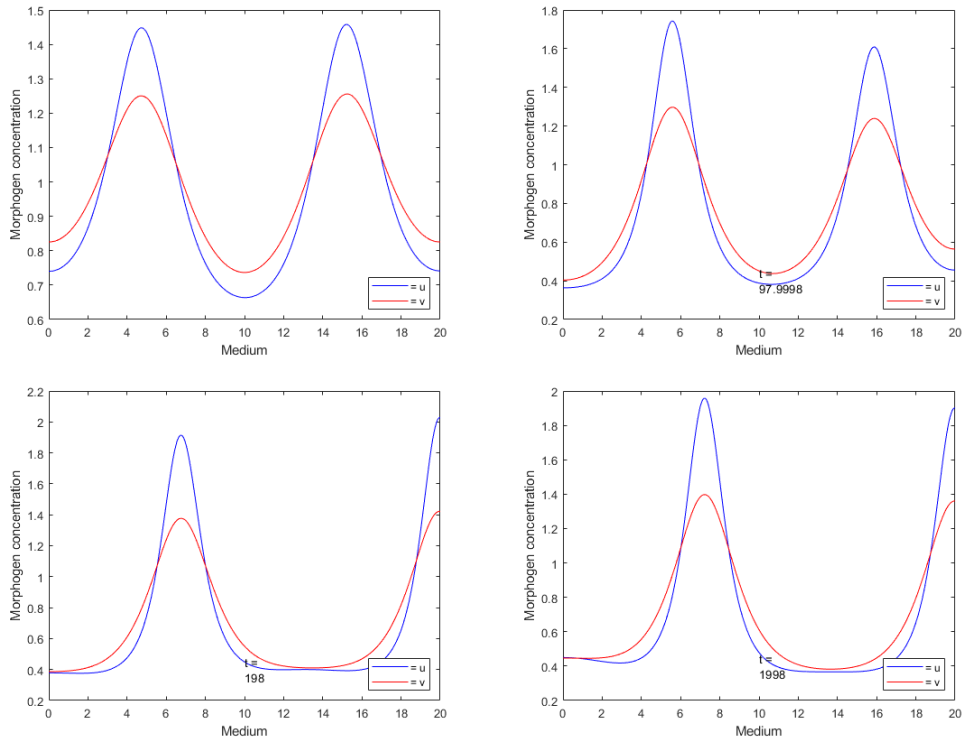

Figure 9: Simulations of the advection time utilising an upwind scheme for advection, taken at $t = 20, 100, 200, 2000$ respectively for upper left, upper right, lower left, lower right. Note that the scheme remains stable in this case, however the result is shifted more and more to the right as time progresses up to a point and is therefore inaccurate. This is most evident in the right hand side of the latter systems, where the right peak collides with the boundary, and remains at it for the remainder of the simulation. This is a result of the way that the upwind scheme simulates points near the boundary: the chemotactic term does not come into play as u_N^j is set as $u_N^j = u_{N-1}^j$ within the simulations for j as simulated, where $N = L/\Delta x$. This means that at the boundary, the result may only decrease with diffusion. The constants in this equation are given by $a = 4.02$, $b = 0.1$, $D = 2$

First off, while the numerics remain stable as the simulation progresses, their accuracy is questionable due to the trend in the middle part of the simulations for the peaks generated to shift rightwards until the boundary is met. As

the simulations start off, two peaks arise from the local disturbances created by the model, clearly visible at $t = 20$. At this stage, these peaks resemble any others generated in previous simulations however as time progresses, we start to see an asymmetry arise between the left and the right peak. This is caused due to the right peak hitting into the medium boundary and becoming drawn towards it, as a result of having relatively fewer points to rely on, making the result for advection less accurate. This is noticeable at $t = 100$, and continues until around $t = 200$ when the right peak becomes centred on the right boundary of the medium. Because of this, the advection term is no longer able to be properly influence the growth of the right peak, and it remains mostly stable in size and remains in position on the boundary. The system now evolves very slowly in time and can be considered stable, although the left peak moves very slowly rightwards as can be observed at time $t = 2000$. Overall, this result is not very useful for accurately simulating the behaviour of the non-constant chemotaxis model in section 2.3 and as such was discarded.

Similar issues can be expected to occur for downwind simulations of advection, therefore these two simple numerical methods have been rejected for simulations of non-constant chemotaxis. This leaves central difference as a potential method for simulating advection under FTCS, although it too runs into problems.

3.2.4 Limitations: Stability

Unlike the upwind and downwind schemes for advection, the central difference scheme does not demonstrate a clear bias for either the left or the right of the medium, at least not by looking at the discretisation grid, however this is insufficient for the scheme to be stable and accurate for the forward time central space scheme. At the very least, stability should first be demonstrated for systems displaying advection under the scheme. Performing analysis for this end however demonstrates the opposite: that such a system is always unstable regardless of step size ratios or applicable coefficients. Further on, the same issues will be demonstrated for the stability of the downwind scheme, by utilising Neumann stability analysis.

Previous von Neumann stability analysis has shown that for diffusive-termed systems, the Forward Time Central Space scheme remains stable, which we have used to establish the stability of the systems in sections 2.1 and 2.2

as the only partial differential terms in space included in them were second order. However, as the advection term causes the generation of first order PDE terms in space, a von Neumann stability analysis is necessary for such a system driven by advection. To this end, we create and solve a simplified advection problem along the lines of the heat equation problem solved for earlier in this section. Let us start by defining our problem as:

$$u_t = -au_x,$$

where a is a constant. The explicit solution for u is easy to compute ($u = f(x - at)$, where $f(x - at)$ is some unknown function), and represents a solution to a wave propagation problem where the wave propagates along the x axis in the positive direction. As we have already derived a temporal scheme, as well as a central difference scheme for 1PDEs in 71, we may substitute them here under the previously developed discretisation grid:

$$u_i^{j+1} = u_i^j - a\left(\frac{\Delta t}{2(\Delta x)^2}\right)(u_{i+1}^j - u_{i-1}^j).$$

Having obtained the numerical scheme for our advection equation, we may finally move onto analysing its stability. Just as we had done for the heat equation, we make a substitution of η_i^j for our term u_i^j, where η_i^j corresponds to the local error of the given coordinate, or in other words the modulus of the difference between the numerically approximated value for u_i^j and its analytical solution at the x and t values corresponding to the discretisation coordinates i and j respectively. Furthermore, we had also obtained a Fourier series substitution during the numerical stability analysis of the heat equation which is applicable here due to both systems occurring on a finite, non-periodic spatial boundary:

$$\eta_i^j = f(i\Delta x - aj\Delta t) - u_i^j, \qquad \eta_i^j = C_k(t)e^{kx\sqrt{-1}}, \tag{72}$$

where k represents the wave number $\frac{\pi}{L}$. The reason for the utilisation of $\sqrt{-1}$ is that i and j have already been assigned roles in this notation. Substitution into the advection equation gives:

$$\begin{aligned} C_k(t + \Delta t)e^{kx\sqrt{-1}} =& C_k(t)e^{kx\sqrt{-1}} \\ &- a\left(\frac{\Delta t}{2(\Delta x)^2}\right)(C_k(t)e^{k(x+\Delta x)\sqrt{-1}} - C_k(t)e^{k(x-\Delta x)\sqrt{-1}}), \end{aligned}$$

which can then be simplified by dividing by $C_k(t)e^{kx\sqrt{-1}}$ to give us the amplification factor for the advection equation.

$$\frac{C_k(t + \Delta t)}{C_k(t)} = 1 - a\left(\frac{\Delta t}{2(\Delta x)^2}\right)(e^{k\Delta x\sqrt{-1}} - e^{-k\Delta x\sqrt{-1}}),$$

which we will call G. G may also be called the Courant condition for stability. In order for the system to be stable, the absolute size of G must be less than one. If it is not, the inaccuracies generated will compound and lead to an unstable result. As we had done before, we will utilise exponential identities for trigonometric functions to simplify the result:

$$G = 1 - a\left(\frac{\Delta t}{(\Delta x)^2}\right)(\sqrt{-1}sin(k\Delta x).$$

Because we are considering the absolute value of G, and the advection corresponding term is strictly imaginary, our result for $|G|$ must always be greater than 1, its real component. This is regardless of the size of a, except for the trivial result of $a = 0$, which would eliminate the advection term entirely. As such, we have to conclude that the forward time central space scheme is unconditionally unstable for advection terms, as is therefore unsuitable for modelling the non-constant chemotactic system in section 2.3. Consequently, alternative schemes were needed to be explored for its simulation. In the following subsection, such schemes were explored, specifically Lax methods.

First however, we may consider the same stability analysis for upwind and downwind schemes. Recalling the upwind and downwind schemes, given by the following equation, for upwind and downwind respectively:

$$u_i^{j+1} = u_i^j \mp a\frac{\Delta t}{\Delta x}(u_i^j - u_{i\mp1}^j).$$

We may make the same substitution of 72 to obtain the following system, where the same reasons for utilising $\sqrt{-1}$ apply as before:

$$C_k(t - \Delta t)e^{kx\sqrt{-1}} = C_k(t)e^{kx\sqrt{-1}} \mp a\frac{\Delta t}{\Delta x}(e^{kx\sqrt{-1}} - e^{k(x\mp\Delta x)\sqrt{-1}})C_k(t).$$

As we had done before, we may cancel this down to obtain the Courant condition, G, given by:

$$G = 1 \mp a\frac{\Delta t}{\Delta x}(1 - e^{\mp\Delta xk\sqrt{-1}}).$$

The condition for stability utilising G is $|G| \leq 1$ therefore we will square both sides of the equation, utilising once again the complex exponential form of cosine:

$$|G|^2 = 1 \mp 2a\frac{\Delta t}{\Delta x}(1 - e^{\mp\Delta xk\sqrt{-1}}) + a^2\left(\frac{\Delta t}{\Delta x}\right)^2 e^{\mp\Delta xk\sqrt{-1}}(-2 + 2cos(\Delta xk)),$$

which eventually becomes the following relation:

$$|G|^2 = 1 - 2a\frac{\Delta t}{\Delta x}\left(\pm 1 - a\frac{\Delta t}{\Delta x}\right)(1 - cos(\Delta x k)) \leq 1.$$

Consider the right-most bracket. Because of the values that cosine may take, this bracket will always remain positive. As a result, after subtracting 1 from both sides to have the inequality be ≤ 0, we may divide by $-2(1-cos(\Delta x k))$ to obtain a more simplified form of the Courant condition for upwind and downwind schemes respectively:

$$a\frac{\Delta t}{\Delta x}\left(\pm 1 - a\frac{\Delta t}{\Delta x}\right) \geq 0.$$

From this condition, it is evident that upwind schemes remain stable so long as $0 \leq a\frac{\Delta t}{\Delta x} \leq 1$ is assured, while downwind schemes remain unconditionally unstable. This result further solidifies the conclusion reached in the previous subsection that the upwind and downwind schemes are inadequate for simulating advection terms for our equation (remember that both stability and accuracy are needed for a scheme to be reliable). As previously mentioned, this discounts the three finite difference schemes for modelling advection, and as such an alternative scheme is considered in the following subsection, namely the two-step Lax Friedrichs method which relies on a staggered discretisation grid, and uses five points instead of two or three to obtain its numerics for advection.

3.3 Lax methods

Having failed to obtain a stable advection approach under the forward time central space scheme, we will instead attempt a lax method. The lax method we will be relying upon, the two-step Lax–Friedrichs method, relies upon the substitution of coordinates at half steps on the grid space (called "staggered grids"), which leads to a greater number of points being needed to simulate each next point than in the previously looked at approaches. For instance, the central difference method relied on two points for the first step,while we will eventually obtain five for the advection. In order to obtain the numerical simulation for this, let us consider just the advection term from the system analysed in section 2.3, in one spatial dimension and rewritten into a more useful form:

$$u_t = -a(uv_x)_x,$$

where v represents a second morphogen. In this subsection, we will concern ourselves with establishing a two-step Lax Friedrichs numerical scheme for

the above equation admissible under a forward time central space scheme, along the lines of the methods presented in [5], in order so that it may then be used to simulate the equation problem in section 2.3. We will start off by noting that the forward time approximation would still need to hold, therefore the simulation would take the form of equation 3.2.2 on page 39:

$$u_i^{j+1} = u_i^j - a\Delta t(u_i^j(v_i^j)_x)_x.$$

From this numerical approximation, we may start to form a Lax approximation for the system. Firstly we make substitutions for u_i^j and v_i^j to separate them into their respective half-terms. Note that because v exists only as a first order differential term and will end up being called one step behind as a result of the method employed for u, we can instead use a central approximation for it on a half step, as it serves the same role:

$$u_i^j = \hat{u}_{i+\frac{1}{2}}^j + \hat{u}_{i-\frac{1}{2}}^j, \quad (v_i^j)_t = \frac{v_{i+\frac{1}{2}}^j - v_{i-\frac{1}{2}}^j}{\Delta x},$$

which is then substituted into the equation to obtain the following. The result was also turned from a differential equation into a difference equation in the outermost x partial differential:

$$u_i^{j+1} = u_i^j - \frac{a\Delta t}{\Delta x}\left(\frac{v_{i+1}^j - v_i^j}{\Delta x}\hat{u}_{i+\frac{1}{2}}^j - \frac{v_i^j - v_{i-1}^j}{\Delta x}\hat{u}_{i-\frac{1}{2}}^j\right).$$

We must now find a way to approximate our values for $\hat{(u)}$. We can do this for each $\hat{u}_i^j$ by considering two values derived from either side of u_i, for which we do have coordinates. We shall call them u_i^- and u_i^+ respectively, from left to right. The exact values they hold is given by the u_i term they correspond to, from which is subtracted the difference between them and the next closest point to $\hat{u}_i^j$ this side of the discretisation grid. As equations, they are given by:

$$u_{i+\frac{1}{2}}^+ = u_{i+1} - \frac{u_{i+2} - u_{i+1}}{2}, \quad u_{i+\frac{1}{2}}^- = u_i - \frac{u_{i-1} - u_i}{2},$$

where j, the time grid coordinate, has been removed from notation for now for clarity. We may use these results to define substitutions for $\hat{u}$, given by the following result, where α is later found to be zero, as as such is removed from the system in the second step:

$$\begin{aligned}\hat{u}_{i+\frac{1}{2}}^j =& \left(u_{i+\frac{1}{2}}^+ + u_{i+\frac{1}{2}}^- + \alpha(u_{i+\frac{1}{2}}^+ - u_{i+\frac{1}{2}}^-) \div v_{i+\frac{1}{2}}\right) \div 2, \\ =& \frac{u_{i+2} + u_{i+1} + u_{i-1} + u_i}{4}.\end{aligned}$$

In order to find values of $\hat{u}^j_{i-\frac{1}{2}}$, one must only go back one step in space, that is subtract 1 from every i. As such, we may now make our final substitution of terms for $\hat{u}$ into the numerical scheme to obtain the final version of the Lax scheme with all morphogens being in full step values:

$$\begin{aligned} u_i^{j+1} =& u_i^j \\ &- \frac{a\Delta t}{(2\Delta x)^2}(v^j_{i+1} - v^j_i)(u_{i+2} + u_{i+1} + u_{i-1} + u_i) \\ &+ \frac{a\Delta t}{(2\Delta x)^2}(v^j_i - v^j_{i-1})(u_{i+1} + u_i + u_{i-2} + u_{i-1}), \end{aligned}$$

which allows us to move forward with numerical stability analysis. However, first we should expand on the parameter α introduced previously. At that time, we had taken α to be zero, though it was not explained nor expanded upon what α was: it actually represents numerical dissipation, and is given by:

$$\alpha = max\left|au_x\right|.$$

Because we already have a term for numerical dissipation in the numerical scheme developed for the system in section 2.2 (the diffusion terms), utilising α is not required. Recall the FTCS scheme developed in the previous subsection for the constant chemotaxis equation (equation 68), omitting the chemotactic term. Onto this equation we will add the chemotactic component developed under the Lax scheme:

$$\begin{aligned} u_i^{j+1} =& u_i^j + D\frac{\Delta t}{(\Delta x)^2}(u^j_{i+1} + u^j_{i-1} - 2u^j_i) + b\Delta t u^j_i(1 - u^j_i) \\ &- \frac{a\Delta t}{(2\Delta x)^2}(v^j_{i+1} - v^j_i)(u_{i+2} + u_{i+1} + u_{i-1} + u_i) \\ &+ \frac{a\Delta t}{(2\Delta x)^2}(v^j_i - v^j_{i-1})(u_{i+1} + u_i + u_{i-2} + u_{i-1}), \\ v_i^{j+1} =& v_i^j + \frac{\Delta t}{(\Delta x)^2}(v^j_{i+1} + v^j_{i-1} - 2v^j_i) + \Delta t(u^j_i - v^j_i), \end{aligned}$$

which completes the numerical scheme for the system of equations in section 2.3.

Conclusion

In the preceding section numerous models for numerical simulations of problems considered analytically in section 2 were considered, as well as advantages and problems associated with them. Firstly a brief introduction into

the methods employed in numerical simulations was given on the basis of a forward time Euler equation which was later used to expand onto the Forward Time Centred Space (FTCS) scheme which was the centrepiece of the numerical simulations employed in this dissertation. This included the demonstrations of limitations and considerations made in the simulations of numerical systems such as the conditionality of stability on factors such as the time step or the implicity or explicity of the system. This was further built upon in the analysis of Forward Time Centred Space systems where the von Neumann method of stability analysis was employed to determine whether the scheme was stable for the admitted orders of differential equations. It was found that while stability was conditional for second order systems (which formed the basis of subsections 2.1 and 2.2), it was unconditionally unstable for systems including first order spatial terms for the central difference and downwind schemes. The issue was eventually solved by the utilisation of a Lax method, for which simulations which were both accurate and stable were obtained. Considered too were upwind and downwind schemes for numerical simulation of the problematic advection term, however these were demonstrated to be, if not unstable for the upwind method, then sufficiently inaccurate to discard.

4 Conclusion

In this dissertation studies explored in [13] were expanded upon from those concerning only reaction-diffusion systems to those displaying chemotaxis both constant and non-constant, under the general umbrella of the Keller-Segel model for the given kinetics and modes of chemotaxis. The biological processes from which chemotaxis arises were explored, with a brief account of the actions deployed by bacteria to move (specifically the E. coli bacterium) were found to be caused by chemotaxis. The E. coli bacterium uses the gradient between the concentrations of a stimulant at one point against another to influence the rate at which is switched from moving, or "running", to turning, or "tumbling".

Analysed too were the Keller-Segel models for analytical stability, in a process not too dissimilar to the one utilised in [13], albeit involving a chemotactic term which had not been the base before, leading to different conclusions with respect to the stability of the solutions and their potential to generate patterns. In all, three models were analysed. The first model was found to, while being capable of pattern generation, lead to rapidly growing morphogen concentrations which led to the model being modified with a logistic term to limit their growth. This was the basis of the second model which was also flawed on account of negative values for u being present leading to its simulations failing, except for when conditions for pattern formation were barely met. This was remedied with the third and final model, which used non-constant chemotaxis to fix this issue. The specific reason for why the issue arose was that for a negative u, the equation in u_t had no terms which could go positive under the influence of u once they all went negative.

The final part of this discretisation was concerned with obtaining numerical simulations for the models tested above, demonstrating the derivation of such systems for the models presented, and analysing the stability and accuracy issues which arose. The Forward Time Central Space scheme was found to be adequate for simulating constant chemotaxis problems, given an adequately small step size which was confirmed, however issues arose for non-constant chemotaxis for the FTCS scheme. The scheme was found to be unconditionally unstable for standard central difference and downwind approximations, and inaccurate for upwind methods by numerical simulation. An alternate method was found and demonstrated via the two-step Lax Friedrichs method as described in [5], which gave stable and accurate pattern results for appropriate parameters in line with section 2.3.

5 Appendix: MATLAB simulations for numerical schemes used

5.1 FTCS simulations

Non-Logarithmic, successful

```
clear all


%%
%Simulation parameters

L=20;          % medium size
tMax=200;        % time max
D=5.;
dofx=0.05;         % space step size
doft=dofx^2/(2.1*D);         % time step size

nTime=tMax/doft;     % time steps
n=L/dofx+1;          % nr grid points
center=int32(n/2);



%%
%System constants and initial conditions
alpha=5;         % chemotactic strengh
gamma =  1.;
betta =  1.;
rho   =  0.;


Du=3.;       % diffusion coefficient
s12=doft/dofx^2;

uVec=zeros(n,1);
vVec=zeros(n,1);
uSol=zeros(n,1);
vSol=zeros(n,1);
```

```
%inital conditions:
for i=1:n
    uVec(i)=0.5;
    vVec(i)=0.5;
end
for i=center-5:center+5
    uVec(i)=0.6;
    vVec(i)=0.6;
end



%%
%Numerical simulation of system
t=0;
figure
Q=0:dofx:L; % Defining space
j0=10000;
for j= 1:nTime
    %integration
    for i=2:n-1
        u=uVec(i);
        v=vVec(i);
        uSol(i)=u+ s12*Du*(uVec(i-1)-2*u+uVec(i+1)) ...
  -alpha*s12*(vVec(i-1)-2*v+vVec(i+1))   ...
           +doft*(rho*uVec(i)*(1. - uVec(i)));
        vSol(i)=v                          ...
              +s12*(vVec(i-1)-2*v+vVec(i+1))         ...
           +doft*(betta*uVec(i) - gamma*vVec(i));
    end
    %BCs
    uSol(1)=uSol(2); uSol(n)=uSol(n-1);
    vSol(1)=vSol(2); vSol(n)=vSol(n-1);

     uVec=uSol;
     vVec=vSol;

    if rem(j,j0) == 0
        plot(Q(1:end),uVec,'b',Q(1:end),vVec,'r');
        txt = {'t = ' t}
        text(1,1,txt);
```

```
        drawnow
    end
    t=t+doft;
end
 t2=t;
 for i=2:n-1
     if uVec(i)>0.5
         p2=i*dofx;
     end
 end
```

```
 %%
 %Plot information
xlabel('Medium')
ylabel('Morphogen concentration')
legend({'= u','= v'},'Location','southeast')
title(sprintf('time=%1.2f', tMax), 'fontsize', 16)
```

Non-Logarithmic, unsuccessful

```
clear all


%%
%Simulation parameters

L=20;          % medium size
tMax=100;       % time max
D=5.;
dofx=0.05;         % space step size
doft=dofx^2/(2.1*D);        % time step size

nTime=tMax/doft;    % time steps
n=L/dofx+1;         % nr grid points
center=int32(n/2);
```

```
%%
%System constants and initial conditions
alpha=-2;        % chemotactic strengh
gamma =  1.;
betta =  1.;
rho   =  0.;


Du=5.;      % diffusion coefficient
s12=doft/dofx^2;

uVec=zeros(n,1);
vVec=zeros(n,1);
uSol=zeros(n,1);
vSol=zeros(n,1);
%inital conditions:
for i=1:n
    uVec(i)=0.5;
    vVec(i)=0.5;
end
for i=center-5:center+5
    uVec(i)=0.6;
    vVec(i)=0.6;
end



%%
%Numerical simulation of system
t=0;
figure
Q=0:dofx:L; % Defining space
j0=10000;
for j= 1:nTime
    %integration
    for i=2:n-1
        u=uVec(i);
        v=vVec(i);
```

```
        uSol(i)=u+ s12*Du*(uVec(i-1)-2*u+uVec(i+1)) ...
            -alpha*s12*(vVec(i-1)-2*v+vVec(i+1))   ...
            +doft*(rho*uVec(i)*(1. - uVec(i)));
        vSol(i)=v                                  ...
            +s12*(vVec(i-1)-2*v+vVec(i+1))         ...
            +doft*(betta*uVec(i) - gamma*vVec(i));
    end
    %BCs
    uSol(1)=uSol(2); uSol(n)=uSol(n-1);
    vSol(1)=vSol(2); vSol(n)=vSol(n-1);

     uVec=uSol;
     vVec=vSol;

    if rem(j,j0) == 0
        plot(Q(1:end),uVec,'b',Q(1:end),vVec,'r');
        txt = {'t = ' t}
        text(1,1,txt);
        axis([0  20    -2.5  2.5])
        drawnow
    end
    t=t+doft;
end
 t2=t;
 for i=2:n-1
     if uVec(i)>0.5
         p2=i*dofx;
     end
 end



 %%
 %Plot information
xlabel('Medium')
ylabel('Morphogen concentration')
legend({'= u','= v'},'Location','southeast')
title(sprintf('time=%1.2f', tMax), 'fontsize', 16)
```

Logarithmic, successful

```
clear all


%%
%Simulation parameters

L=20;          % medium size
tMax=200;        % time max
D=2.;
dofx=0.05;         % space step size
doft=dofx^2/(2.1*D);         % time step size

nTime=tMax/doft;     % time steps
n=L/dofx+1;          % nr grid points
center=int32(n/2);



%%
%System constants and initial conditions
alpha=4.02;         % chemotactic strengh
gamma =  1.;
betta =  1.;
rho   =  1.;


Du=1.;       % diffusion coefficient
s12=doft/dofx^2;

uVec=zeros(n,1);
vVec=zeros(n,1);
uSol=zeros(n,1);
vSol=zeros(n,1);
%inital conditions:
for i=1:n
    uVec(i)=0.5;
    vVec(i)=0.5;
end
```

```
for i=center-5:center+5
    uVec(i)=0.6;
    vVec(i)=0.6;
end



%%
%Numerical simulation of system
t=0;
figure
Q=0:dofx:L; % Defining space
j0=10000;
for j= 1:nTime
    %integration
    for i=2:n-1
        u=uVec(i);
        v=vVec(i);
        uSol(i)=u+ s12*Du*(uVec(i-1)-2*u+uVec(i+1)) ...
        -alpha*s12*(vVec(i-1)-2*v+vVec(i+1))   ...
            +doft*(rho*uVec(i)*(1. - uVec(i)));
        vSol(i)=v                                    ...
            +s12*(vVec(i-1)-2*v+vVec(i+1))          ...
            +doft*(betta*uVec(i) - gamma*vVec(i));
    end
    %BCs
    uSol(1)=uSol(2); uSol(n)=uSol(n-1);
    vSol(1)=vSol(2); vSol(n)=vSol(n-1);

     uVec=uSol;
     vVec=vSol;

    if rem(j,j0) == 0
        plot(Q(1:end),uVec,'b',Q(1:end),vVec,'r');
        txt = {'t = ' t}
        text(1,1,txt);
        drawnow
    end
    t=t+doft;
end
 t2=t;
```

```
 for i=2:n-1
     if uVec(i)>0.5
         p2=i*dofx;
     end
 end




 %%
 %Plot information
xlabel('Medium')
ylabel('Morphogen concentration')
legend({'= u','= v'},'Location','southeast')
title(sprintf('time=%1.2f', tMax), 'fontsize', 16)
```

Logarithmic, unsuccessful

```
clear all


%%
%Simulation parameters

L=20;          % medium size
tMax=200;       % time max
D=5.;
dofx=0.05;         % space step size
doft=dofx^2/(2.1*D);        % time step size

nTime=tMax/doft;    % time steps
n=L/dofx+1;         % nr grid points
center=int32(n/2);



%%
%System constants and initial conditions
alpha=1.02;        % chemotactic strengh
```

```
gamma =  1.;
betta =  1.;
rho   =  2.;


Du=5.;      % diffusion coefficient
s12=doft/dofx^2;

uVec=zeros(n,1);
vVec=zeros(n,1);
uSol=zeros(n,1);
vSol=zeros(n,1);
%inital conditions:
for i=1:n
    uVec(i)=0.5;
    vVec(i)=0.5;
end
for i=center-5:center+5
    uVec(i)=0.6;
    vVec(i)=0.6;
end



%%
%Numerical simulation of system
t=0;
figure
Q=0:dofx:L; % Defining space
j0=10000;
for j= 1:nTime
    %integration
    for i=2:n-1
        u=uVec(i);
        v=vVec(i);
        uSol(i)=u+ s12*Du*(uVec(i-1)-2*u+uVec(i+1)) ...
            -alpha*s12*(vVec(i-1)-2*v+vVec(i+1))   ...
            +doft*(rho*uVec(i)*(1. - uVec(i)));
        vSol(i)=v                                  ...
            +s12*(vVec(i-1)-2*v+vVec(i+1))         ...
            +doft*(betta*uVec(i) - gamma*vVec(i));
```

```
    end
    %BCs
    uSol(1)=uSol(2); uSol(n)=uSol(n-1);
    vSol(1)=vSol(2); vSol(n)=vSol(n-1);

     uVec=uSol;
     vVec=vSol;

    if rem(j,j0) == 0
        plot(Q(1:end),uVec,'b',Q(1:end),vVec,'r');
        txt = {'t = ' t}
        text(1,1,txt);
        axis([0 20 0.975 1.025])
        drawnow
    end
    t=t+doft;
end
 t2=t;
 for i=2:n-1
     if uVec(i)>0.5
         p2=i*dofx;
     end
 end




 %%
 %Plot information
xlabel('Medium')
ylabel('Morphogen concentration')
legend({'= u','= v'},'Location','southeast')
title(sprintf('time=%1.2f', tMax), 'fontsize', 16)
```

5.2 Lax simulations

Successful

```
clear all
```

```
%%
%Simulation parameters

L=20;          % medium size
tMax=500;        % time max
D=5.;
dofx=0.05;         % space step size
doft=0.80*dofx^2/(2*D);         % time step size

nTime=tMax/doft;     % time steps
n=L/dofx+1;          % nr grid points
center=int32(n/2);



%%
%System constants and initial conditions
alpha=4.02;         % chemotactic strengh
gamma =  1.;
betta =  1.;
rho   =  .1;


Du=1.;       % diffusion coefficient
s12=doft/dofx^2;
s11=doft/dofx;

uVec=zeros(n,1);
vVec=zeros(n,1);
uSol=zeros(n,1);
vSol=zeros(n,1);
%inital conditions:
for i=1:n
    uVec(i)=1.;
    vVec(i)=1.;
end
for i=center-5:center+5
    uVec(i)=0.5;
    vVec(i)=0.5;
```

```
end



%%
%Numerical simulation of system
t=0;
figure
Q=0:dofx:L; % Defining space
j0=10000;

uPlus = zeros(n-2);
uMinus = zeros(n-2);
vHalf = zeros(n-2);
fHat = zeros(n-1);
for j= 1:nTime
    %integration
    %Lax-Freidricht setup
    for i=2:n-2
        uPlus(i)  = 0.5*(3*uVec(i+1)-uVec(i+2));
    end
    uPlus(n-1) = uVec(n-1);
    for i=2:n-1
        uMinus(i) = 0.5*(3*uVec(i)-uVec(i-1));
        vHalf(i)  = (vVec(i+1)-vVec(i))/dofx;
        fHat(i) = 0.5*((uPlus(i)*vHalf(i))+(uMinus(i)*(vHalf(i))));
    end
    for i=2:n-1
        u=uVec(i);
        v=vVec(i);
        uSol(i)=u+ s12*Du*(uVec(i-1)-2*u+uVec(i+1)) ...
            -alpha*s11*(fHat(i)-fHat(i-1))         ...
            +doft*(rho*uVec(i)*(1. - uVec(i)));
        vSol(i)=v                                  ...
            +s12*(vVec(i-1)-2*v+vVec(i+1))           ...
            +doft*(betta*uVec(i) - gamma*vVec(i));
    end
    %BCs
    uSol(1)=uSol(2); uSol(n)=uSol(n-1);
    vSol(1)=vSol(2); vSol(n)=vSol(n-1);
```

```
     uVec=uSol;
     vVec=vSol;

    if rem(j,j0) == 0
        plot(Q(1:end),uVec,'b',Q(1:end),vVec,'r');
        txt = {'t = ' t}
        text(10,0.4,txt)
        axis([0 20 0 2])
        drawnow
    end
    t=t+doft;
end
 t2=t;
 for i=2:n-1
     if uVec(i)>0.5
         p2=i*dofx;
     end
 end



 %%
 %Plot information
xlabel('Medium')
ylabel('Morphogen concentration')
legend({'= u','= v'},'Location','southeast')
```

Unsuccessful

```
clear all


%%
%Simulation parameters

L=20;          % medium size
tMax=500;       % time max
D=5.;
```

```
dofx=0.05;        % space step size
doft=0.80*dofx^2/(2*D);        % time step size

nTime=tMax/doft;    % time steps
n=L/dofx+1;         % nr grid points
center=int32(n/2);



%%
%System constants and initial conditions
alpha=1.02;        % chemotactic strengh
gamma =  1.;
betta =  1.;
rho   =  2;


Du=1.;      % diffusion coefficient
s12=doft/dofx^2;
s11=doft/dofx;

uVec=zeros(n,1);
vVec=zeros(n,1);
uSol=zeros(n,1);
vSol=zeros(n,1);
%inital conditions:
for i=1:n
    uVec(i)=1.;
    vVec(i)=1.;
end
for i=center-5:center+5
    uVec(i)=0.5;
    vVec(i)=0.5;
end



%%
%Numerical simulation of system
t=0;
figure
```

```
Q=0:dofx:L; % Defining space
j0=10000;

uPlus = zeros(n-2);
uMinus = zeros(n-2);
vHalf = zeros(n-2);
fHat = zeros(n-1);
for j= 1:nTime
    %integration
    %Lax-Freidricht setup
    for i=2:n-2
        uPlus(i)  = 0.5*(3*uVec(i+1)-uVec(i+2));
    end
    uPlus(n-1) = uVec(n-1);
    for i=2:n-1
        uMinus(i) = 0.5*(3*uVec(i)-uVec(i-1));
        vHalf(i)  = (vVec(i+1)-vVec(i))/dofx;
        fHat(i) = 0.5*((uPlus(i)*vHalf(i))+(uMinus(i)*(vHalf(i))));
    end
    for i=2:n-1
        u=uVec(i);
        v=vVec(i);
        uSol(i)=u+ s12*Du*(uVec(i-1)-2*u+uVec(i+1)) ...
            -alpha*s11*(fHat(i)-fHat(i-1))          ...
            +doft*(rho*uVec(i)*(1. - uVec(i)));
        vSol(i)=v                                   ...
            +s12*(vVec(i-1)-2*v+vVec(i+1))          ...
            +doft*(betta*uVec(i) - gamma*vVec(i));
    end
    %BCs
    uSol(1)=uSol(2); uSol(n)=uSol(n-1);
    vSol(1)=vSol(2); vSol(n)=vSol(n-1);

     uVec=uSol;
     vVec=vSol;

    if rem(j,j0) == 0
        plot(Q(1:end),uVec,'b',Q(1:end),vVec,'r');
        txt = {'t = ' t}
        text(10,0.4,txt)
        axis([0 20 0 2])
```

```
        drawnow
    end
    t=t+doft;
end
 t2=t;
 for i=2:n-1
     if uVec(i)>0.5
         p2=i*dofx;
     end
 end
```

```
 %%
 %Plot information
xlabel('Medium')
ylabel('Morphogen concentration')
legend({'= u','= v'},'Location','southeast')
```

5.3 Upwind advection

```
clear all


%%
%Simulation parameters

L=20;          % medium size
tMax=2000;       % time max
D=5.;
dofx=0.05;         % space step size
doft=0.80*dofx^2/(2*D);        % time step size

nTime=tMax/doft;    % time steps
n=L/dofx+1;          % nr grid points
center=int32(n/2);
```

```
%%
%System constants and initial conditions
alpha=4.02;        % chemotactic strengh
gamma =  1.;
betta =  1.;
rho   =  0.1;


Du=2.;      % diffusion coefficient
s12=doft/dofx^2;

uVec=zeros(n,1);
vVec=zeros(n,1);
uSol=zeros(n,1);
vSol=zeros(n,1);
%inital conditions:
for i=1:n
    uVec(i)=1.;
    vVec(i)=1.;
end
for i=center-5:center+5
    uVec(i)=0.5;
    vVec(i)=0.5;
end



%%
%Numerical simulation of system
t=0;
figure
Q=0:dofx:L; % Defining space
j0=10000;
for j= 1:nTime
    %integration
    for i=2:n-1
        u=uVec(i);
        v=vVec(i);
        uSol(i)=u+ s12*Du*(uVec(i-1)-2*u+uVec(i+1))   ...
            -alpha*s12*(((vVec(i+1)-v)*(uVec(i+1)-u))...
            +(u*(vVec(i-1)-2*v+vVec(i+1))))              ...
```

```
            +doft*(rho*uVec(i)*(1. - uVec(i)));
        vSol(i)=v                                       ...
            +s12*(vVec(i-1)-2*v+vVec(i+1))                  ...
            +doft*(betta*uVec(i) - gamma*vVec(i));
    end
    %BCs
    uSol(1)=uSol(2); uSol(n)=uSol(n-1);
    vSol(1)=vSol(2); vSol(n)=vSol(n-1);

     uVec=uSol;
     vVec=vSol;

    if rem(j,j0) == 0
        plot(Q(1:end),uVec,'b',Q(1:end),vVec,'r');
        txt = {'t = ' t}
        text(10,0.4,txt)
        drawnow
    end
    t=t+doft;
end
 t2=t;
 for i=2:n-1
     if uVec(i)>0.5
         p2=i*dofx;
     end
 end



 %%
 %Plot information
xlabel('Medium')
ylabel('Morphogen concentration')
legend({'= u','= v'},'Location','southeast')
```

References

[1] Gurusamy Arumugam, André H. Erhardt, Indurekha Eswaramoorthy, and Balachandran Krishnan. Existence of weak solutions to the keller–segel chemotaxis system with additional cross-diffusion. *Nonlinear Analysis: Real World Applications*, 54, 2020.

[2] CASPER HL Beentjes. Pattern formation analysis in the schnakenberg model. Technical report, Technical Report, University of Oxford, UK, 2015.

[3] H.C. Berg and D.A. Brown. Chemotaxis in escherichia coli analysed by three-dimensional tracking. *Nature*, 239(5374):500–504, 1972.

[4] Edward A. Codling, Michael J. Plank, and Simon Benhamou. Random walk models in biology. *JOURNAL OF THE ROYAL SOCIETY INTERFACE*, 5(25):813 – 834, 2008.

[5] Gurgen Dallakyan. Numerical simulations for chemotaxis models. *Biomath Communications*, 6:16, 05 2019.

[6] Bassam Elgamoudi. Effect of c-di-gmp on biofilm formation and motility of campylobacter jejun. 10 2014.

[7] Javier Fernández de Cañete, Cipriano Galindo, and Inmaculada García Moral. *System engineering and automation. an interactive educational approach.* Springer, 2011.

[8] Erwin W Gelfand. Importance of the leukotriene b4-blt1 and ltb4-blt2 pathways in asthma. *Seminars in immunology*, 33:44 – 51, 2017.

[9] A. Gierer and H. Meinhardt. A theory of biological pattern formation. *Kybernetik*, 12(1):30, 1972.

[10] Preethee Gonpot, Joseph Collet, and Noor Sookia. Gierer-meinhardt model: Bifurcation analysis and pattern formation. *Trends in Applied Sciences Research*, 3:115–128, 02 2008.

[11] Nigel Clifford Harrison. *MODELLING CHEMOTACTIC MOTION OF CELLS IN BIOLOGICAL TISSUE WITH APPLICATIONS TO EMBRYOGENESIS*. PhD thesis, University of Liverpool.

[12] Evelyn F. Keller and Lee A. Segel. Model for chemotaxis. *Journal of Theoretical Biology*, 30(2):225–234, 1971.

[13] Arwid Kuks. Turing patterns. Master's thesis, University of Liverpool.

[14] K. W. Morton and D. F. Mayers. *Numerical solution of partial differential equations : an introduction.* Cambridge University Press, 2005.

[15] J. D. Murray and J. D. Murray. *Mathematical Biology. II: Spatial Models and Biomedical Applications.* Springer New York, 2003.

[16] Buividovich P. Euler method for numerical solution of ordinary differential equations, 2021. Accessed 2021-11-15.

[17] Amit Kumar Rana, Yang Li, Qiujie Dang, and Fan Yang. Monocytes in rheumatoid arthritis: Circulating precursors of macrophages and osteoclasts and, their heterogeneity and plasticity role in ra pathogenesis. *International Immunopharmacology*, 65:348–359, 2018.

[18] Manan'Iarivo Rasolonjanahary. Scaling of morphogenetic patterns in continuous and discrete models. 2013.

[19] Christina H Stuelten, Carole A Parent, and Denise J Montell. Cell motility in cancer invasion and metastasis: insights from simple model organisms. *Nature reviews. Cancer*, 18(5):296 – 312, 2018.

[20] A. M. Turing. The chemical basis of morphogenesis. *Philosophical Transactions B: Biological Sciences*, 237(641):37 – 72, 1952.

[21] Junhua Yuan, Karen A. Fahrner, Linda Turner, and Howard C. Berg. Asymmetry in the clockwise and counterclockwise rotation of the bacterial flagellar motor. *Proceedings of the National Academy of Sciences*, 107(29):12846–12849, 2010.